ENVISAT GOMOS Monthly report: May 2004

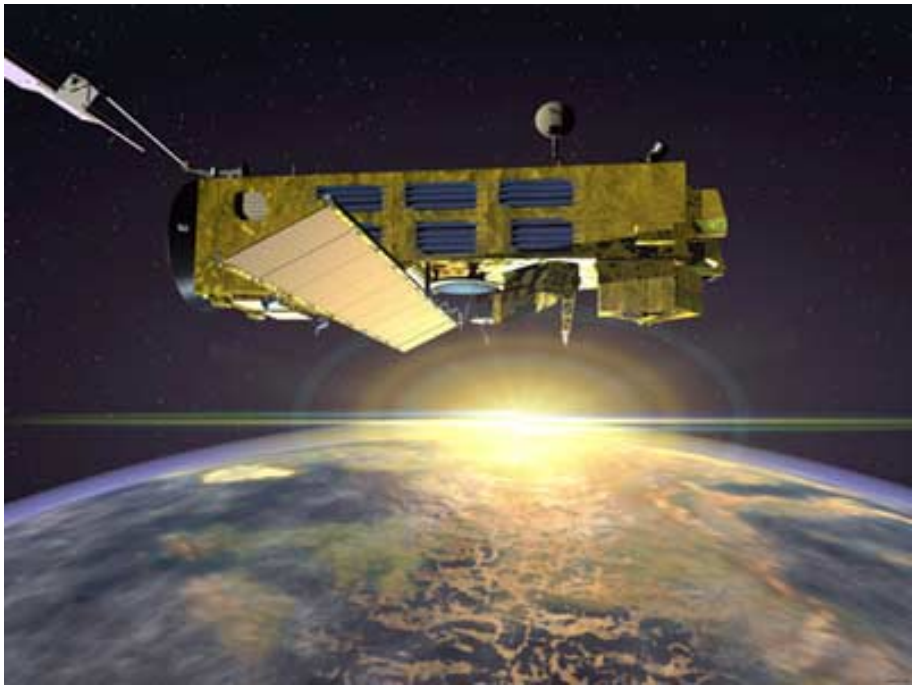

Prepared by:	PCF Team	ESA EOP-GOQ
Inputs from:	GOMOS Quality Working Group	

Issue:	1.0
Reference:	ENVI-SPPA-EOPG-TN-04-0017
Date of issue:	6 July 2004
Status:	Reviewed
Document type:	Technical Note
Approved by:	Pascal Lecomte, Rob Koopman

TABLE OF CONTENTS

1 INTRODUCTION

The GOMOS monthly report documents the current status and recent changes to the GOMOS instrument, its data processing chain, and its data products.
The Monthly Report (hereafter MR) is composed of analysis results obtained by the Product Control Facility, combined with inputs received from the different entities working on GOMOS operation, calibration, product validation and data quality. These teams participate in the GOMOS Quality Working Group:

- European Space Agency (ESRIN-PCF, ESOC, ESTEC-PLSO)
- ACRI
- Service d'Aeronomie
- Finnish Meteorological Institute
- IASB-Belgian Institute for Space Aeronomy
- Astrium Space
- ECMWF

In addition, the group interfaces with the Atmospheric Chemistry Validation Team.

1.1 Scope

The main objective of the Monthly Report is to give, on a regular basis, the status of GOMOS instrument performance, data acquisition, results of anomaly investigations, calibration activities and validation campaigns. The following six sections compose the MR:

- Summary
- Unavailability
- Instrument Performance and Configuration
- Level 1 Product Quality Monitoring
- Level 2 Product Quality Monitoring
- Validation Activities and Results

1.2 References

[1] ENVISAT Weekly Mission Operations Report #91, #92, #93, #94 ENVI-ESOC-OPS-RP-1011-TOS-OF
[2] 'Level 1b Detailed Processing Model', PO-RS-ACR-GS-0001, issue 6.1, 28 Nov, 2003
[3] 'Level 2 Detailed Processing Model', PO-RS-ACR-GS-0002, issue 6.0, 6 Feb, 2004

1.3 Acronyms and Abbreviations

ACVT Atmospheric Chemistry Validation Team
ADF Auxiliary Data File

ADS	Auxiliary Data Server
ANX	Ascending Node Crossing
ARF	Archiving Facility (PDS)
CCU	Central Communication Unit
CFS	CCU Flight Software
CNES	Centre National d'Études Spatiales
CTI	Configuration Table Interface / Configurable Transfer Item
CR	Cyclic Report
DC	Dark Charge
DMOP	Detailed Mission Operation Plan
DPM	Detailed Processing Model
DS	Data Server
DSA	Dark Sky Area
DSD	Data Set Descriptor
ECMWF	European Centre for Medium Weather Forecast
EQSOL	Equipment Switch Off Line
ESA	European Space Agency
ESL	Expert Support Laboratory
ESRIN	European Space Research Institute
ESTEC	European Space Research & Technology Centre
ESOC	European Space Operations Centre
FCM	Fine Control Mode
FMI	Finnish Meteorological Institute
FOCC	Flight Operations Control Centre (ENVISAT)
FP1	Fast Photometer 1
FP2	Fast Photometer 2
GADS	Global Annotations Data Set
GOMOS	Global Ozone Monitoring by Occultation of Stars
GOPR	GOmos PRototype
GS	Ground Segment
HK	Housekeeping
IASB	Institut d'Aeronomie Spatiale de Belgique
IAT	Interactive Analysis Tool
ICU	Instrument Control Unit
IDL	Interactive Data Language
IECF	Instrument Engineering and Calibration Facilities
IMK	Institute of Meteorology Karlsruhe (Meteorologisch Institut Karlsuhe)
INV	Inventory Facilities (PDS)
IPF	Instrument Processing Facilities (PDS)
JPL	Jet Propulsion Laboratory
LAN	Local Area Network
LMA	Levenberg-Marquardt Algorithm
LPCE	Laboratoire de Physique et Chimie de l'Environnement
LUT	Look Up Table
MCMD	Macro Command
MDE	Mechanism Drive Electronics
MIP	Most Illuminated Pixel
MPH	Main Product Header

MPS	Mission Planning System
MR	Monthly Report
OBT	On Board Time
OCM	Orbit Control Manoeuvre
OOP	Out-of-plane
OP	Operational Phase of ENVISAT
PAC	Processing and Archiving Centre (PDS)
PCF	Product Control Facility
PDCC	Payload Data Control Centre (PDS)
PDHS	Payload Data Handling Station (PDS)
PDHS-E	Payload Data Handling Station – ESRIN
PDHS-K	Payload Data Handling Station – Kiruna
PDS	Payload Data Segment
PEB	Payload Equipment Bay
PLSOL	Payload Switch off Line
PMC	Payload Module Computer
PRNU	Pixel Response Non Uniformity
PSO	On-Orbit Position
QC	Quality Control
QUARC	Quality Analysis and Reporting Computer
QWG	Quality Working Group
RIVM	Rijksinstituut voor Volksgezondheid en Milieu
RTS	Random Telegraphic Signal
SA	Service d'Aeronomie
SAA	South Atlantic Anomaly
SATU	Star Acquisition and Tracking Unit
SFA	Steering Front Assembly
SFCM	Stellar Fine Control Mode
SFM	Steering Front Mechanism
SMNA	Servicio Meteorológico Nacional de Argentina
SODAP	Switch On and Data Acquisition Phase
SPA1	Spectrometer A CCD 1
SPA2	Spectrometer A CCD 2
SPB1	Spectrometer B CCD 1
SPB2	Spectrometer B CCD 2
SPH	Specific Product Header
SQADS	Summary Quality Annotation Data Set
SSP	Sun Shade Position
SZA	Solar Zenith Angle

2 SUMMARY

During the reporting month GOMOS instrument had one planned unavailability period on 6th May 22:50 until 7th May 02:24. For the rest of the month, GOMOS has been operating nominally (section 3.1).

The level 0 availability is very high during the month even if a decrease is seen by the end of the month. For level 1 data there is a gradual decrease at the end of the reporting period arriving to almost 90% of availability during the last week of May (section 3.3).

The detector temperatures during May are 0.5 degrees greater than the ones registered in April. The expected seasonal variation of the temperatures with amplitude of around one degree can be clearly observed (section 4.2).

The standard deviation of the modulation signal presents high values after the inclusion, at the end of March, of the ESRIN level 0 data. Although it is to be confirmed, it is suspected that the South Atlantic Anomaly is the cause of these unexpected peaks. The quality of ESRIN data, in particular over the SAA zone, is thus under investigation (section 4.4.2).

The elevation MIP has a significant variation till 12th December 2003 when a new PSO algorithm was activated in order to reduce the deviations of the ENVISAT platform attitude with respect to the nominal one. The amplitude of the MIP displacement seems now to be much smaller confirming that the algorithm is working as expected (section 4.5.3).

The variation of the radiometric sensitivity ratio is outside the threshold for some photometer ratios and for some stars. Values outside the warning threshold set to 10% are observed for the photometers, and investigations were performed by the QWG. An inaccurate reflectivity correction LUT was suspected to be the cause of the increase but a new one is in use since 12th February 2004 and some ratios are already outside the threshold. New investigations have shown that the increase could be related to the fact that the occultation illumination condition starts to include twilight/straylight. To verify this, the computation of the ratios will be performed using only occultations in full dark conditions and compared to the previous results (section 5.4.1).

From this monthly report onwards, new information on quality flags is included: section 5.2 for level 1b data and section 6.2 for level 2 data.

On 18th and 26th May new calibration ADF's were disseminated with updated DC maps of orbits 11561 and 11689 respectively (section 5.1.2).

3 INSTRUMENT UNAVAILABILITY

3.1 GOMOS Unavailability Periods

In table 3.1-1 there is a list of GOMOS unavailability reports issued during the period 1st May (00:00:00) until 31st May 2004. For roughly 3.5 hours GOMOS was unavailable due to a manoeuvre between 6th and 7th of May.

Table 3.1-1: List of unavailability periods issued during the reporting month

Reference of unavailability report	Start time Star orbit	Stop time Stop orbit	Description
EN-UNA-2004/0131	6 May 2004 22:50:00.000 Orbit = 11421	7 May 2004 02:24:00.000 Orbit = 11423	FCM Maint for 7 May 2004

3.2 Stars Lost in Centering

The acquisition of a star initiates with a rallying phase where the telescope mechanism is directed towards the expected position of the star. Subsequently the acquisition procedure enters into detection mode, where the SATU star tracker output signal is pre-processed for spot presence survey and for the location of the most illuminated couple of adjacent pixels for two added lines, over the detection field. The Most Illuminated Pixel (MIP) defines the position of the first SATU centering window. The next step in the acquisition sequence is then initiated and consists of a centering phase where the SATU output signal is pre-processed for spot presence survey over the maximum of 10x10 pixel field. This allows the third phase to begin: the tracking phase.

The centering phase has occasionally resulted in loss of the star from the field of view. The fig. 3.2-1 reports the percentage of the stars lost in centering for the period 03-FEB-2003 to 30-MAY-2004. It can be seen that three stars, mainly weak stars (higher star id means higher magnitude) are lost during centering phase between 4 and 7 % of their planned observations. The star id 115 was lost in 40% of the times but it was planned to be occulted five times and was lost twice (in period 26th January – 1st February), so this high percentage of loss is not statistically significant.

As the monitoring shows neither trend nor excessively high percentages of loss, there is no need for the moment to reject any star from the catalogue, and there is no indication of instrument-related problems.

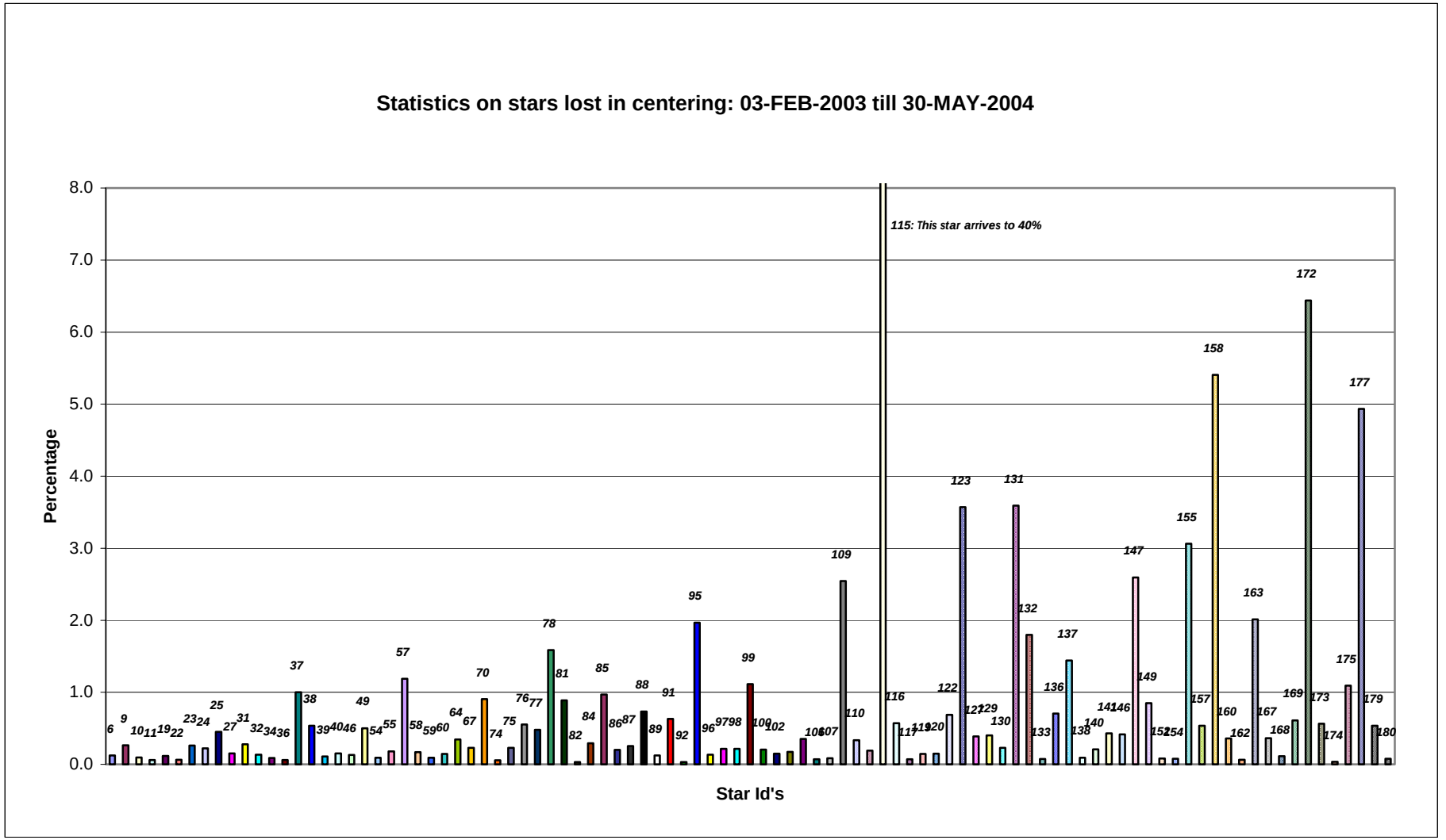

Figure 3.2-1: Statistics on stars that have been lost during the centering phase. The number above the columns correspond to the Star I

3.3 Data Generation Gaps

The trend in percentage of available data within the archives PDHS-K and PDHS-E is depicted in fig. 3.3-1 (when instrument was in operation). It is a good indicator on how the PDS chain is working in terms of generation and dissemination of data to the archives. The percentage is calculated once per week.

The level 0 availability is very high during the month even if a decrease is seen by the end of the month. For level 1 data there is a gradual decrease at the end of the reporting period arriving to almost 90% of availability during the last week of May.

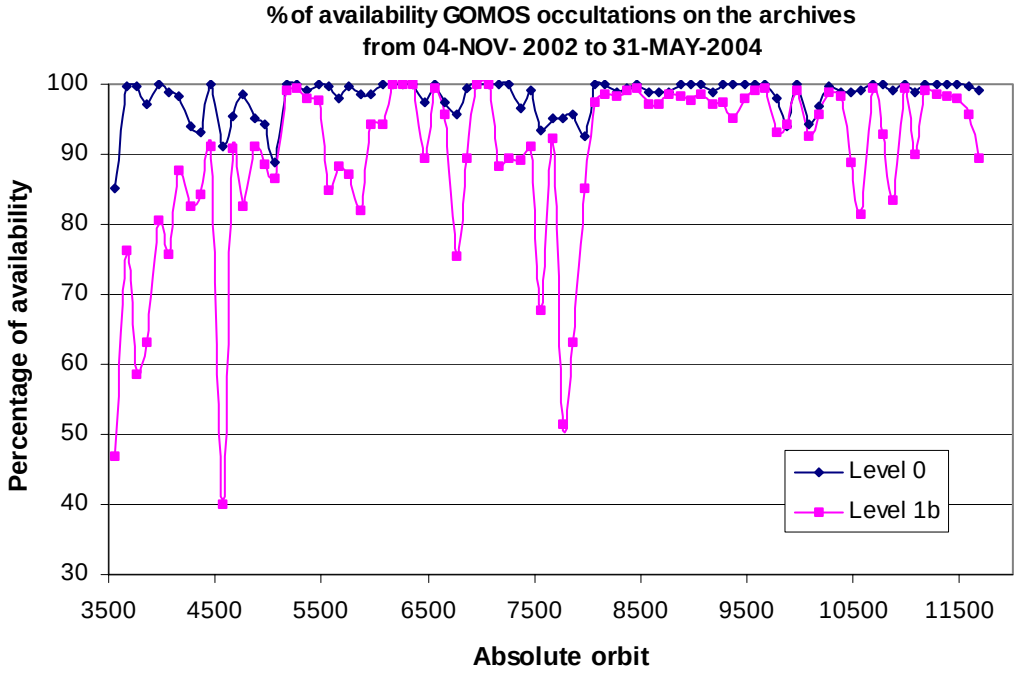

Figure 3.3-1: Percentage of level 0 and level 1b data availability on the archives PDHS-E and PDHS-K

3.3.1 LEVEL 0 PRODUCTS: GOM_NL__0P

Occultations planned to be acquired but for which no GOM_NL__0P data product has become available are presented in fig. 3.3-2 for the reporting month.

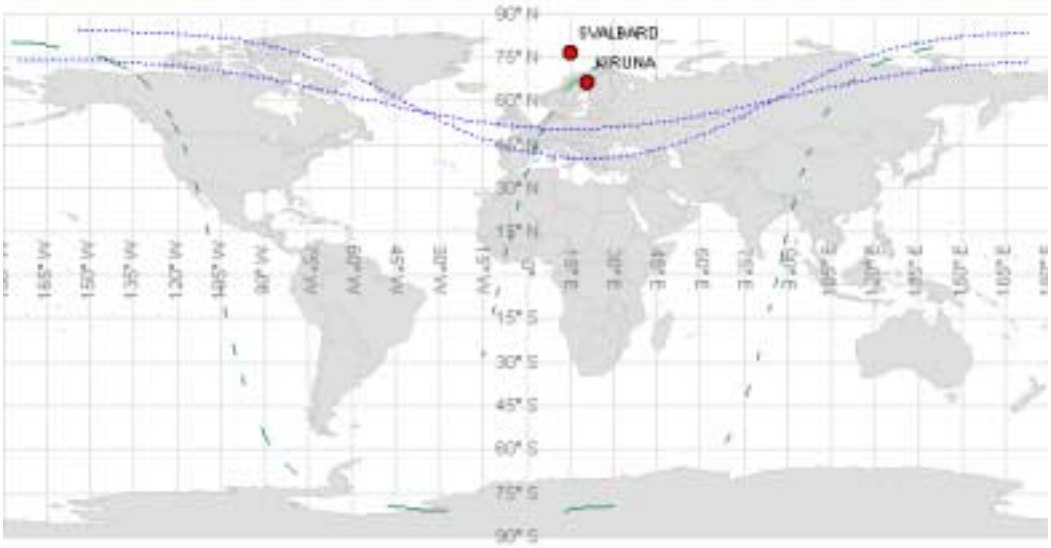

Figure 3.3-2: The green lines are the orbit segments corresponding to planned data acquisitions for which no GOMOS level 0 product has become available. The blue dashed curve represents the visibility of Kiruna and Svalbard acquisition stations

3.3.2 HIGHER LEVEL PRODUCTS

Routine dissemination of higher-level products produced by the PDS to Cal/Val teams and other users is enabled. Currently ESA provides the Cal/Val teams with selected products that are generated with the prototype processor developed and operated by ACRI.

4 INSTRUMENT CONFIGURATION AND PERFORMANCE

4.1 Instrument Operation and Configuration

During the period end of March 2003 to July 2003 the azimuth range had to be decreased in steps (table 4.1-1) to avoid an instrument problem ("Voice_coil_command_saturation" anomaly) that caused GOMOS to go into STAND BY/REFUSE mode. On July 2003 the driver assembly was switched to the redundant B-side and since that date the full azimuth range (-10.8, +90.8) is again available.

Table 4.1-1: Historical changes in Azimuth configuration

Date	Orbit	Minimum Azimuth	Maximum Azimuth
29-MAR-2003 17:40	5635	0.0	+90.8
31-MAY-2003 06:22	6530	+4.0	+90.8
16-JUN-2003 16:17	6765	+12.0	+90.8
15-JUL-2003 01:39	7200	-10.8	+90.8

The operations of the instrument in other modes than occultation mode are identified in table 4.1-2.

There was no new Configurable Table Interface (CTI) uploaded to the instrument. The files used since the beginning of the mission are in table 4.1-3.

Table 4.1-2: GOMOS operations during the reporting month

UTC time	Start orbit	Stop orbit	Mode (Asynchronous or Synchronous)	Calibration (CAL) or Dark Sky Area (DSA)
01 May 2004 15:19:58	11345	11345	A	DSA101
08 May 2004 06:36:51	11440	11447	A	CAL61
15 May 2004 14:39:44	11545	11545	A	DSA102
22 May 2004 14:19:36	11645	11645	A	DSA103
29 May 2004 13:59:29	11745	11745	A	DSA104

Table 4.1-3: Historic CTI Tables

CTI filename	Dissemination to FOCC
CTI_SMP_GMVIEC20030716_123904_00000000_00000004_20030715_000000_20781231_235959.N1	16-JUL-2003
CTI_SMP_GMVIEC20021104_075734_00000000_00000003_20021002_000000_20781231_235959.N1	06-NOV-2003
CTI_SMP_GMVIEC20021002_082339_00000000_00000002_20021002_000000_20781231_235959.N1	07-OCT-2003
CTI_SMP_GMVIEC20020207_154455_00000000_00000000_20020301_032709_20781231_235959.N1	21-FEB-2002

4.2 Thermal Performance

Since the beginning of the mission the hot pixel and RTS phenomena are producing a continuous increase of the dark charge signal within the CCD detectors (see section 4.4.1). In order to minimize this effect, three successive CCD cool down were performed in orbits 800 (25th April 2002), 1050 (13th May 2002) and 2780 (11th September 2002) with a total decrease in temperature of 14 degrees.

Fig. 4.2-1 and 4.2-2 display, respectively, the overall temperature variation and the temperature variation around the Ascending Node Crossing (ANX) time with a resolution of 0.4 degrees (coding accuracy for level 0 data). The CCD temperatures during May are 0.5 degrees greater than the ones registered in April. The expected seasonal variation of the temperatures with amplitude of around one degree can be clearly observed and also a slight global increase due to the radiator ageing. The peaks that occur mainly in spectrometer B1 and B2 are also to be noted. They happen a little before the ANX for some consecutive orbits and every 8-10 days. Their origin is still not known, as we did not find any correlation between these peaks and other activities carried out by other ENVISAT instruments. The CCD temperature at almost the same latitude location (fig. 4.2-2) is monitored in order to detect any inter-orbital temperature variation.

The decrease observed on 24th March 2003, twice in September 2003 and at the beginning of December 2003 in all detectors is after GOMOS switch off periods, when the instrument did not have enough time to reach the nominal temperature before starting the measurements.

The orbital temperature variation of the detector SPB2 (fig. 4.2-3 & 4.2-4) is a little bit bigger that the nominal (the nominal is around 2 degrees) being the maximum difference around 3 degrees. The stability of the temperature during the orbit is important because it affects the position of the interference patterns.

The phenomenon of the interference is present mainly in SPB and this Pixel Response Non-Uniformity (PRNU) is corrected during the processing.

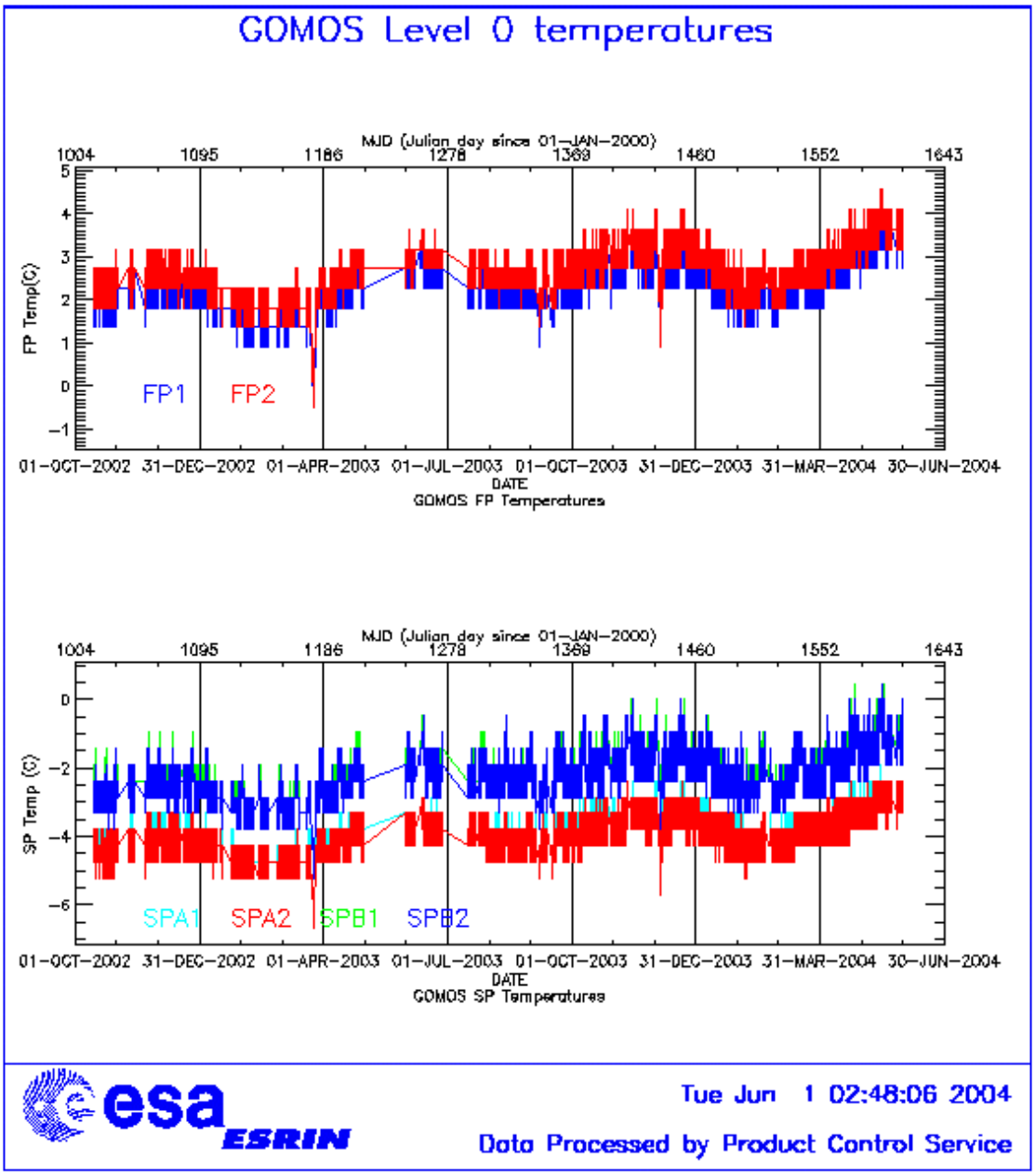

Figure 4.2-1: Level 0 temperature evolution of all GOMOS CCD detectors since October 2002 until the end of the reporting month

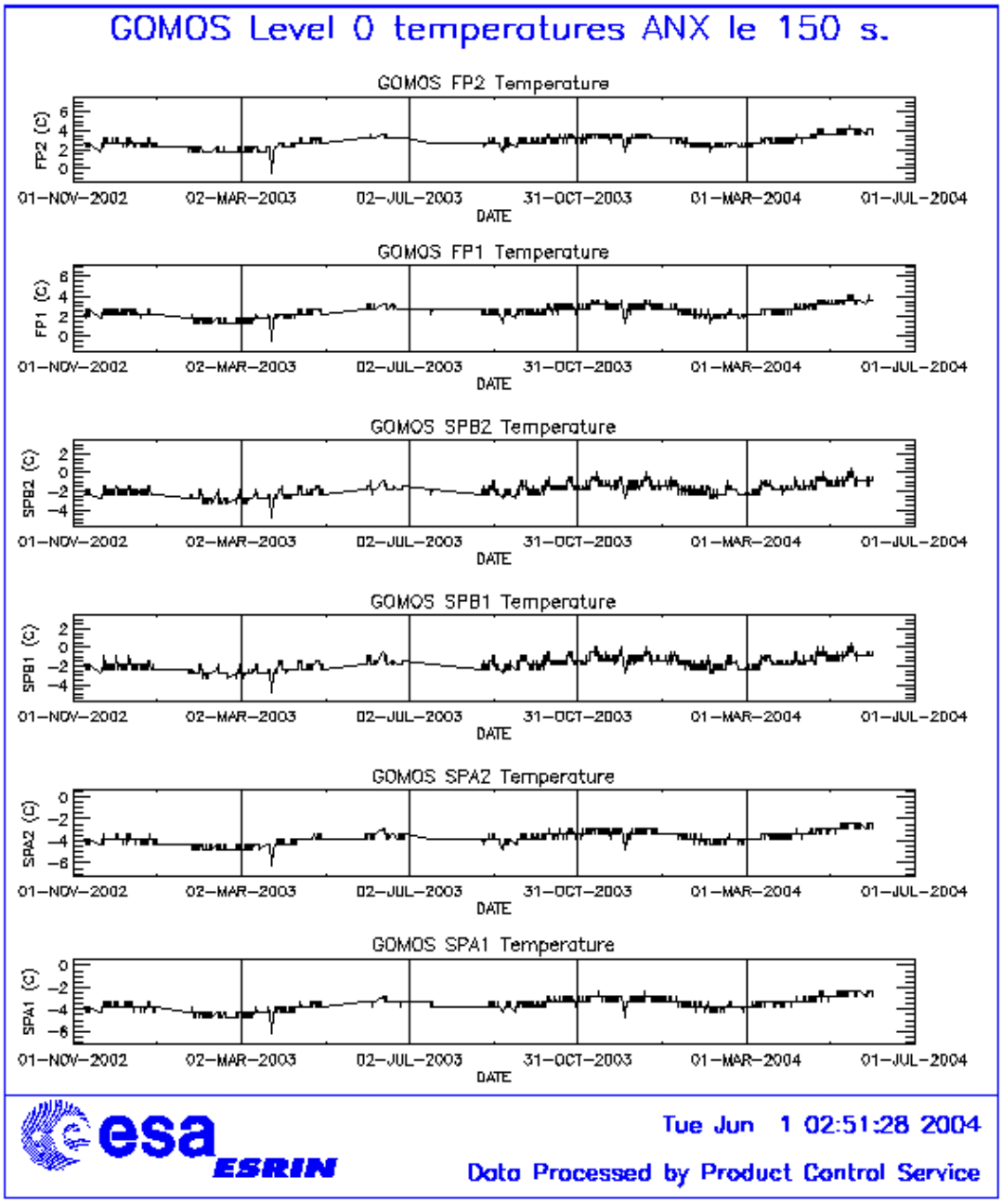

Figure 4.2-2: **Level 0 temperature evolution of all GOMOS CCD detectors around ANX since November 2002 until the end of the reporting month**

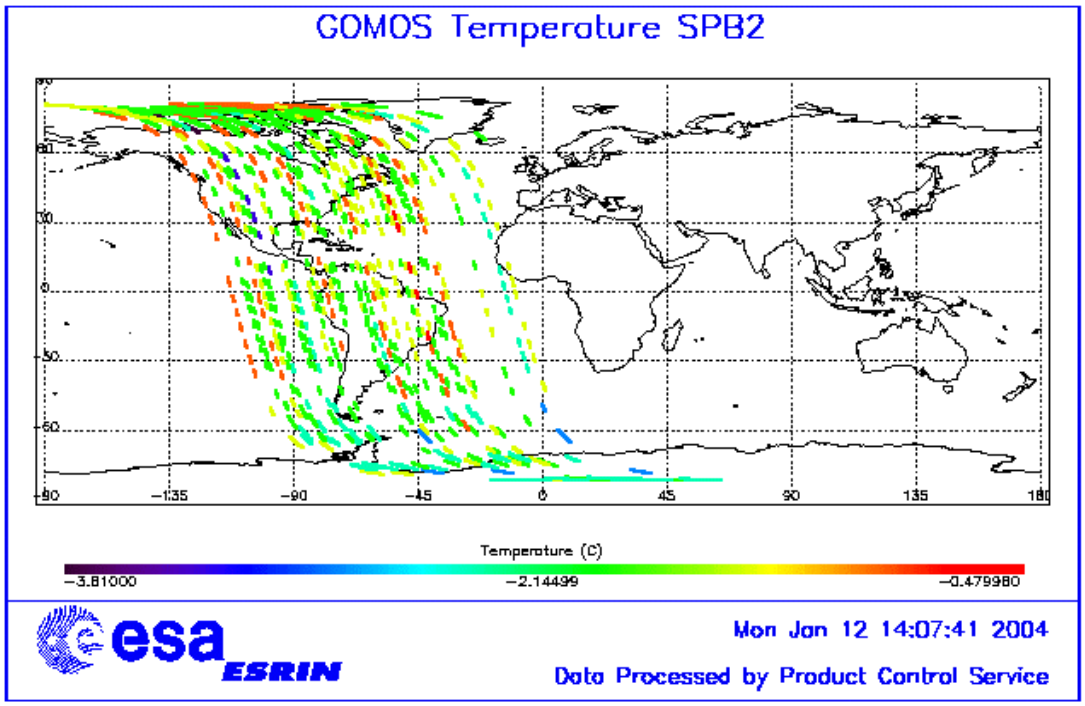

Figure 4.2-3: Ascending orbital variation of SPB2 temperature during some orbits on May 2004

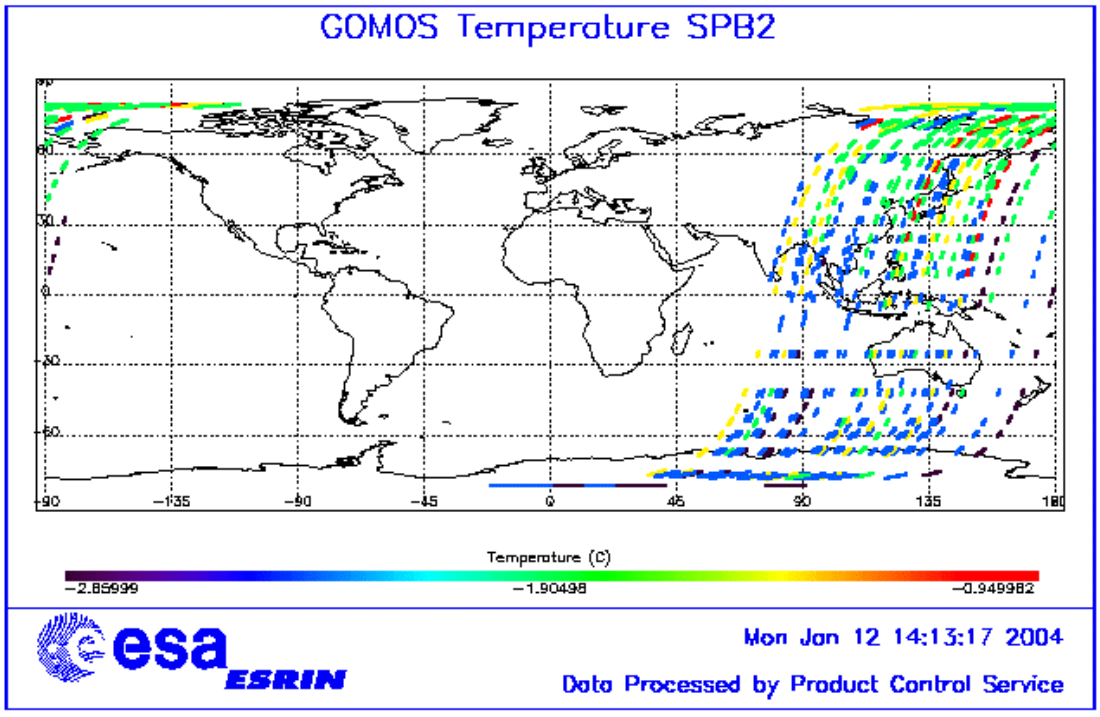

Figure 4.2-4: Descending orbital variation of SPB2 temperature during some orbits on May 2004

4.3 Optomechanical Performance

No new band setting calibration has been performed during May. The last one has been done on April.

- Version GOMOS/4.00 and previous ones:

In the processors versions of GOMOS GOMOS/4.00 and previous the spectra is expected to be aligned along CCD lines, and therefore use only a single average line index per CCD. In table 4.3-1 the mean values of the location of the star signal for all the calibration analysis done are reported. The 'left' and 'right' values are calculated (the whole interval is not used) because the spectra present a slight slope, more pronounced in the spectrometer B (see fig. 4-3.1). In table 4.3-2, mean values of the location of the star signal are calculated for some specific wavelength intervals. These intervals have been changed between the calibration performed in September 2002 and the ones performed afterwards (until November 2003). Table 4.3-3 reports the average location of the star spot on the photometer 1 and 2 CCD.

- Version GOMOS/4.02:

In the actual processor version (GOMOS/4.02) operational since 23rd March 2004, a Look Up Table (LUT) gives the line index of the spectra location as a function of the wavelength (blue dots in fig. 4.3-1). A new calibration exercise has been performed during April. The position of the stellar spectra of star id 31, 18 and 4 observed in dark-limb spatial spread monitoring mode have been averaged above 120 km altitude and compared to the values of the LUT. The results confirm the LUT values (see table 4.3-4) so for the time being there is no need to update the LUT.

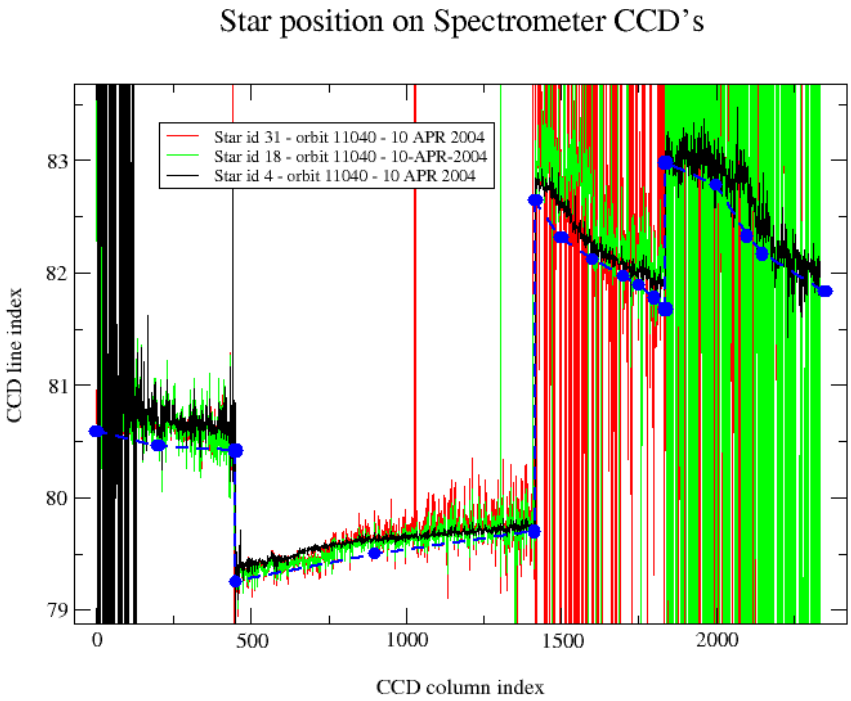

Figure 4.3-1: Average position of star spectra on the CCD

Table 4.3-1: Mean value of the location of the star signal during the occultation at the edges of every band (mean over 50 values, filtering the outliers)

	UV (SPA1) left/right	VIS (SPA2) left/right (Inverted spectra)	IR1 (SPB1) left/right	IR2 (SPB2) left/right
11/09/2002	80.7/80.7	79.8/79.5	82.8/81.9	83.1/82.1
01/01/2003	80.7/80.6	79.8/79.5	82.8/82.0	83.2/82.2
17/07/2003 & 02/08/2003	80.7/80.7	79.8/79.5	82.8/81.9	83.1/82.1
08/11/2003	80.7/80.6	79.8/79.5	82.8/81.9	83.1/82.1

Table 4.3-2: Mean value of the location of the star signal during the occultation (as table 4.3-1) but now within some wavelength intervals

	UV (SPA1)	VIS (SPA2)	IR1 (SPB1)	IR2 (SPB2)
11/09/2002 wl range (nm)	80.8 [300-330]	79.8 [500-530]	82.6 [760-765]	82.9 [937-942]
01/01/2003 wl range (nm)	80.6 [350-360]	78.6 [650-670]	81.6 [760-765]	80.3 [935-945]
02/08/2003	80.6	79.7	82.5	82.8
08/11/2003	80.6	79.9	82.4	82.8

Table 4.3-3: Average column and row pixel location of the star spot on the photometer CCD during the occultation

	FP1 (column/row)	FP2 (column/row)
11/09/2002	11/4	5/5
01/01/2003	10/4	6/4.9
02/08/2003	10/4	6/5
08/11/2003	10/4	6/5

Table 4.3-4: Location of the star signal on the CCD's (corresponding to fig. 4.3-1)

Pixel Column	LUT (Pixel line)	Calibration on 10-APR-2004
0	**80.59**	80.80
20	**80.46**	80.60
449	**80.42**	80.50
450	**79.25**	79.39
900	**79.50**	79.63
1415	**79.70**	79.76
1416	**82.64**	82.80
1500	**82.31**	82.60
1600	**82.12**	82.22
1700	**81.97**	82.04
1750	**81.89**	81.98
1800	**81.78**	81.91
1835	**81.68**	81.88
1836	**82.98**	83.10
2000	**82.78**	82.90
2100	**82.33**	82.70
2150	**82.17**	82.40
2350	**81.83**	82.00

4.4 Electronic Performance

4.4.1 DARK CHARGE EVOLUTION AND TREND

The trend of Dark Charge (DC) is of crucial importance for the final quality of the products, and is therefore subject to intense monitoring. As part of the DC there is:

- "Hot pixels", a pixel is "hot" when its dark charge exceeds its value measured on ground, at the same temperature, by a significant amount.
- RTS phenomenon (Random Telegraphic Signal), it is an abrupt change (positive or negative) of the CCD pixel signal, random in time, affecting only the DC part of the signal and not the photon generated signal.

The temperature dependence of the DC would make this parameter a good indicator of the DC behaviour, but the hot pixels and the RTS are producing a continuous increase of the DC (see trend in fig. 4.4-1 and 4.4-2). To take into account these phenomena, since version GOMOS/4.00 (actual one is GOMOS/4.02) a DC map per orbit is extracted from a Dark Sky Area (DSA) observation performed around ANX (full dark conditions). For every level 1b product (occultation), the actual thermistor temperature of the CCD is used to convert the DC map measured around ANX into an estimate of the DC at the time (and different temperature) of the actual occultation. When the DSA observation is not available, the DC map inside the calibration product that was measured at a given thermistor reference temperature is used; again, the actual thermistor temperature of the CCD is used to compute the actual map. Table 4.4-1 reports the list of products that used the DC maps inside the calibration file due to the non-availability of DSA observation. A "CAL DC map with no T dep." means that, as the temperature information was not available for the occultation, the DC map used is exactly the one inside the Calibration product.

Table 4.4-1: Table of level 1b products that used the Calibration DC maps instead of the DSA observation

Product name	DC information
GOM_TRA_1PNPDE20040504_020434_000000442026_00304_11380_0000.N1	DC map with no T dep. (12)
GOM_TRA_1PNPDE20040504_021055_000000402026_00304_11380_0001.N1	DC map used (0)
GOM_TRA_1PNPDE20040504_021307_000000412026_00304_11380_0002.N1	DC map used (0)
GOM_TRA_1PNPDE20040504_021505_000000452026_00304_11380_0003.N1	DC map used (0)
GOM_TRA_1PNPDE20040504_021746_000000432026_00304_11380_0004.N1	DC map used (0)
GOM_TRA_1PNPDE20040504_021916_000000422026_00304_11380_0005.N1	DC map used (0)
GOM_TRA_1PNPDE20040504_022230_000000662026_00304_11380_0006.N1	DC map used (0)
GOM_TRA_1PNPDE20040507_022832_000000682026_00347_11423_0000.N1	DC map with no T dep. (12)
GOM_TRA_1PNPDE20040511_014204_000000462026_00404_11480_0000.N1	DC map with no T dep. (12)
GOM_TRA_1PNPDE20040511_014535_000000442026_00404_11480_0001.N1	DC map used (0)
GOM_TRA_1PNPDE20040511_015120_000000442026_00404_11480_0002.N1	DC map used (0)
GOM_TRA_1PNPDE20040511_015333_000000412026_00404_11480_0003.N1	DC map used (0)
GOM_TRA_1PNPDE20040511_015522_000000522026_00404_11480_0004.N1	DC map used (0)
GOM_TRA_1PNPDE20040511_015713_000000592026_00404_11480_0005.N1	DC map used (0)
GOM_TRA_1PNPDE20040511_015947_000000412026_00404_11480_0006.N1	DC map used (0)
GOM_TRA_1PNPDE20040511_020303_000000682026_00404_11480_0007.N1	DC map used (0)
GOM_TRA_1PNPDE20040518_012246_000000432027_00003_11580_0000.N1	DC map with no T dep. (12)
GOM_TRA_1PNPDE20040518_012424_000000392027_00003_11580_0001.N1	DC map used (0)

GOM_TRA_1PNPDE20040518_012641_000000452027_00003_11580_0002.N1	DC map used (0)
GOM_TRA_1PNPDE20040518_013147_000000422027_00003_11580_0003.N1	DC map used (0)
GOM_TRA_1PNPDE20040518_013357_000000422027_00003_11580_0004.N1	DC map used (0)
GOM_TRA_1PNPDE20040518_013536_000000462027_00003_11580_0005.N1	DC map used (0)
GOM_TRA_1PNPDE20040518_013720_000000532027_00003_11580_0006.N1	DC map used (0)
GOM_TRA_1PNPDE20040518_013911_000000412027_00003_11580_0007.N1	DC map used (0)
GOM_TRA_1PNPDE20040518_014041_000000422027_00003_11580_0008.N1	DC map used (0)
GOM_TRA_1PNPDE20040525_010228_000000462027_00103_11680_0000.N1	DC map with no T dep. (12)
GOM_TRA_1PNPDE20040525_010428_000000372027_00103_11680_0001.N1	DC map used (0)
GOM_TRA_1PNPDE20040525_010746_000000452027_00103_11680_0002.N1	DC map used (0)
GOM_TRA_1PNPDE20040525_011208_000000432027_00103_11680_0003.N1	DC map used (0)
GOM_TRA_1PNPDE20040525_011415_000000392027_00103_11680_0004.N1	DC map used (0)
GOM_TRA_1PNPDE20040525_011545_000000422027_00103_11680_0005.N1	DC map used (0)
GOM_TRA_1PNPDE20040525_011807_000000612027_00103_11680_0006.N1	DC map used (0)
GOM_TRA_1PNPDE20040525_011956_000000782027_00103_11680_0007.N1	DC map used (0)

In fig. 4.4-1 and 4.4-2 it is plotted the average DC inserted by the processor into the level 1b data products for the spectrometers SPA1 and SPB2 (per band: upper, central and lower). From the figures, it can be noted that there is an increase of DC for the last month as expected.

The same DC values are plotted in fig. 4.4-3 but for some occultations belonging only to the reporting month.

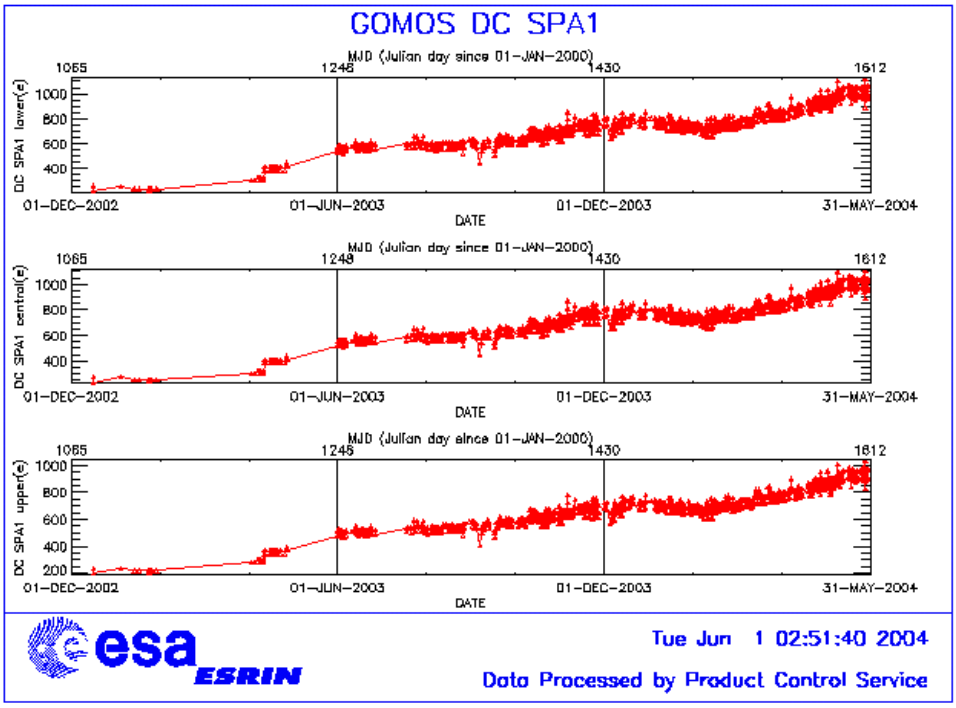

Figure 4.4-1: Mean DC evolution on SPA1 since 15th December 2002 until the end of the reporting month

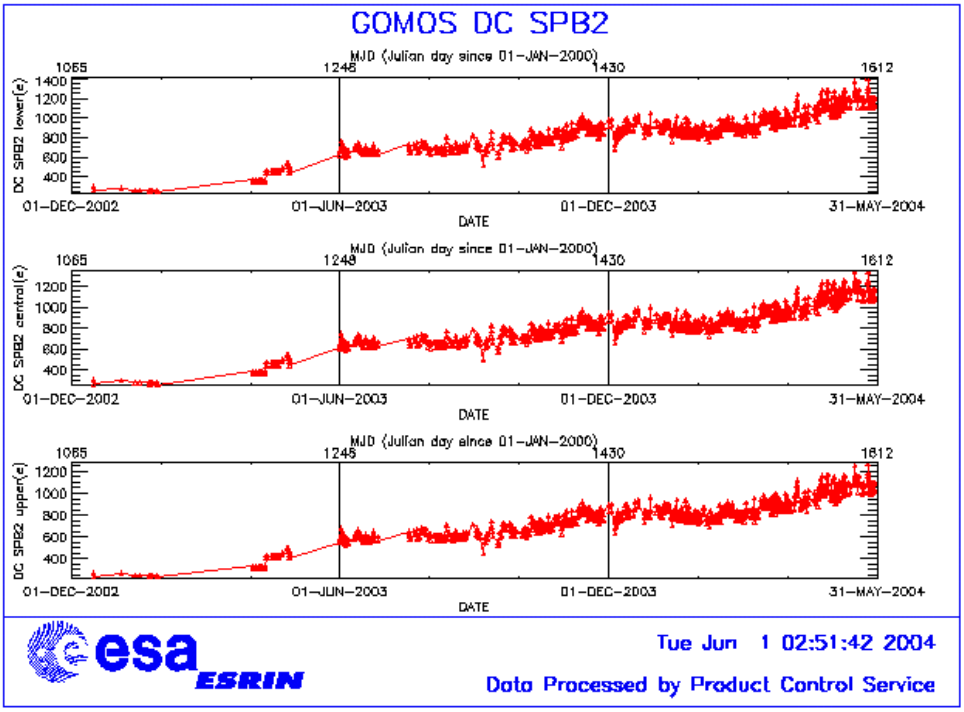

Figure 4.4-2: Mean DC evolution on SPB2 from 15th December 2002 until the end of the reporting month

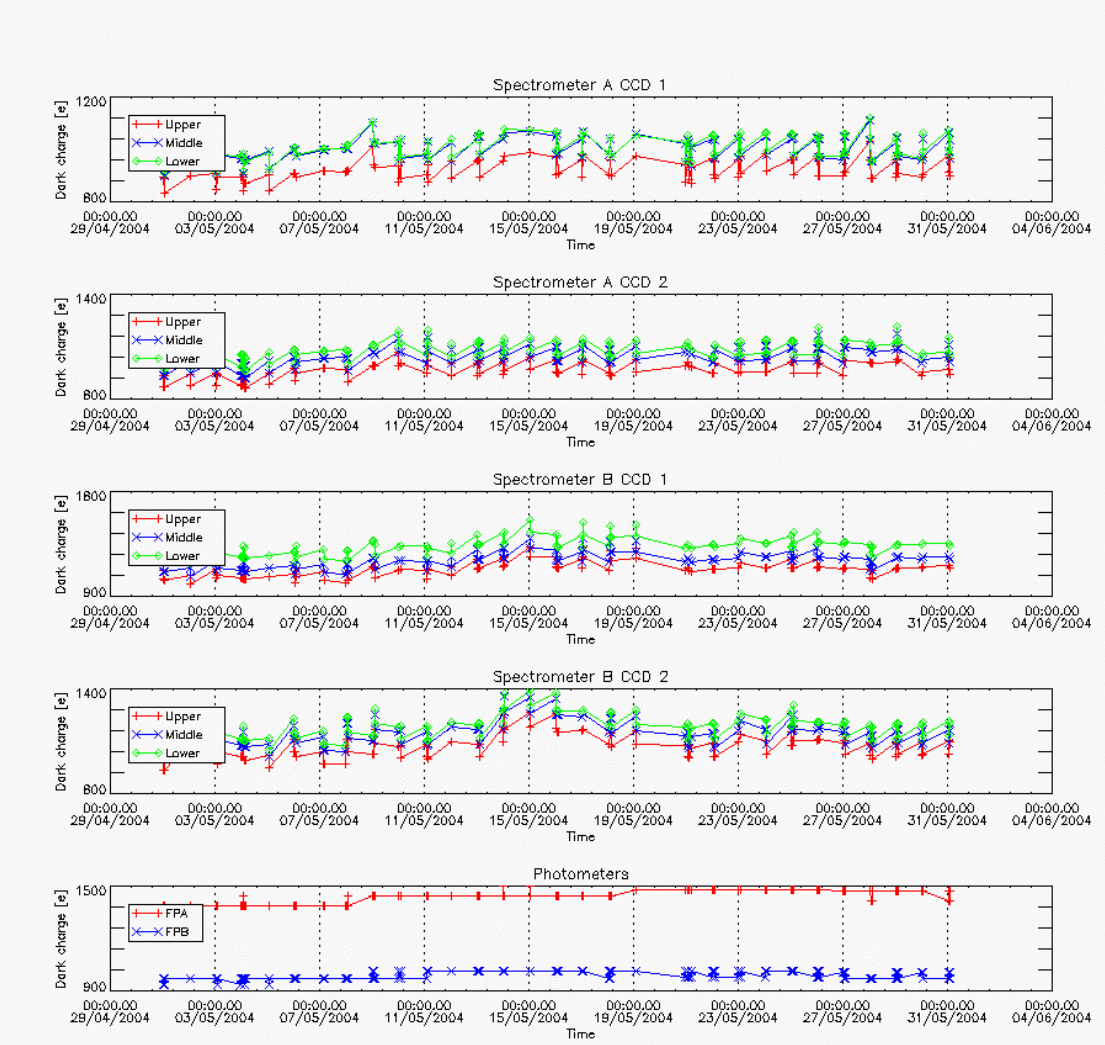

Figure 4.4-3: Mean Dark Charge of spectrometers and photometers during reporting month.

4.4.2 SIGNAL MODULATION

A parasitic signal was found to be systematically present, added to the useful signal, at least for spectrometers A1 and A2. The modulation is corrected in the data processing, but the modulation signal standard deviation is routinely monitored in order to detect any trend (fig. 4.4-4).

The modulation standard deviation, for every spectrometer, is characterised as follows:

$$\sigma_{mod} = (\text{'static noises'} - \text{'total static variance'})^{1/2} / \text{gain} \qquad \text{(in ADU)}$$

- The 'static noises' are calculated from the DSA observation performed once per orbit
- The 'total static variance' is obtained from ADF data (electronic chain noise, quantization noise).

The standard deviation of the modulation signal (fig. 4.4-4) presents high values after the inclusion at the end of March of the ESRIN level 0 data. Although it is to be confirmed, it is suspected that the South Atlantic Anomaly is the cause of these unexpected peaks. The quality of ESRIN data, in particular over the SAA zone, is thus under investigation.

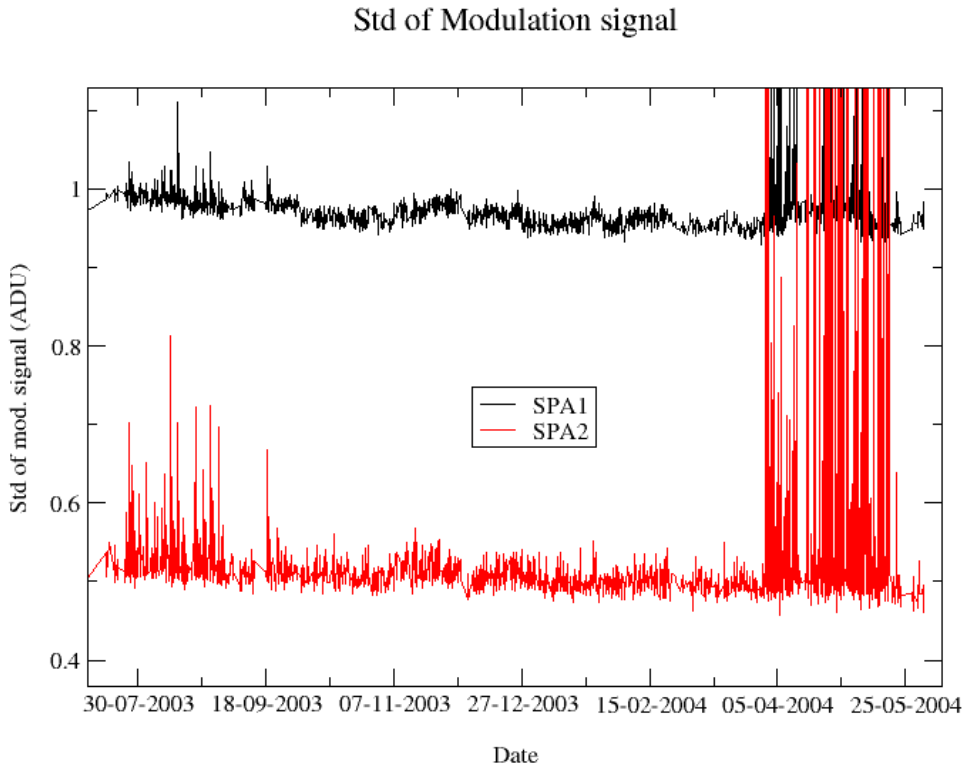

Figure 4.4-4: Standard deviation of the modulation signal

4.4.3 ELECTRONIC CHAIN GAIN AND OFFSET

No new electronic chain gain and offset calibration has been done during the reporting month so these results have been already presented in previous MR.

The routine monitoring of the ADC offset is a good indicator of the ageing of the instrument electronics. During the definition of this routine activity, an exercise has been done to analyze the variation of the ADC offset using the calibration observation in linearity mode (orbits 2810, 4384, 4834, 5219 and 5734). The fig. 4.4-5 presents the evolution of the calibrated ADC offset for each spectrometer electronic chain. The unexpected increase of this offset seems to be due to an external contribution. In the ADC offset calibration procedure, linearity observations are used with two integration times of 0.25 and 0.50 seconds to extrapolate to an integration time of 0 seconds that give the complete chain offset and not only the ADC offset. The complete offset contains any possible offsets, and especially the static dark charge (i.e. the dark charge that does not depend of the spectrometer integration time). If the memory area of the CCD is affected by the generation of hot pixels (this is confirmed by the presence of vertical lines visible

in the measurement maps in spatial spread monitoring mode), it becomes that the increase observed in fig. 4.4-5 is due to these new hot pixels.

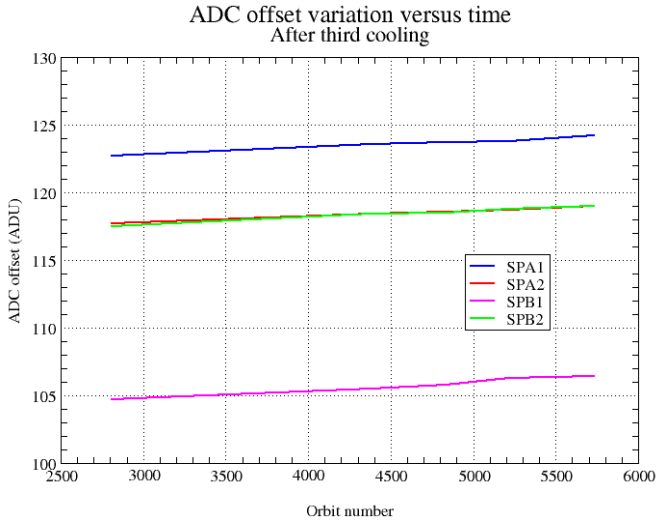

Figure 4.4-5: Evolution of the ADC offset for each spectrometer electronic chain

Next task consists in completing the analysis to confirm that the offset increase is due to the hot pixels in memory area. This can be proven by the study of the noise due to the increased dark charge. The increase of ADC offset will be assumed to be equal to the increase of 'static dark charge' and the corresponding noise will be computed and compared to the increase of the signal variance residual.

If we keep the ADC offset constant, as it is also used to compute the dark charge at band level used to correct the samples in the level 1b processing, the increase of the static dark charge - not taken into account in the ADC offset - is compensated by an artificial increase of the calibrated dark charge. So, the star and limb spectra are correctly corrected for dark charge. A small bias can be added to the instrument noise due to the incorrect dark charge level. Anyway, this quantity is not large enough to require a modification of the ADC offset value.

4.5 Acquisition, Detection and Pointing Performance

4.5.1 SATU NOISE EQUIVALENT ANGLE

The Star Acquisition and Tracking Unit (SATU) noise equivalent angle (SATU NEA) consists of the statistical angular variation of the SATU data above the atmosphere.
The mean of the standard deviation (std over the 50 values per measurement) above 105 km are computed for every occultation, giving two values per occultation: one in the 'X' direction, one in the 'Y' direction. A mean value per day in every direction and limb is calculated and monitored in order to assess instrument performance in terms of star pointing. The thresholds are 2 and 3 micro radians in 'X' and 'Y' directions respectively. Before May 2003, data above 90 km have been considered (instead of 105 km) but from May 2003 on, data taken in the mesospheric oxygen layer (located around 100 km altitude) have

been avoided because they could cause fluctuations on the SATU data. Also the products with errors (error flag set) are discarded from May 2003 onwards.

It can be seen in fig. 4-5.1 that the SATU NEA was very stable during the whole month and well below the thresholds.

The results for some occultations belonging to previous months (monthly averages) are presented in fig. 4.5-2, where no trend is visible so far.

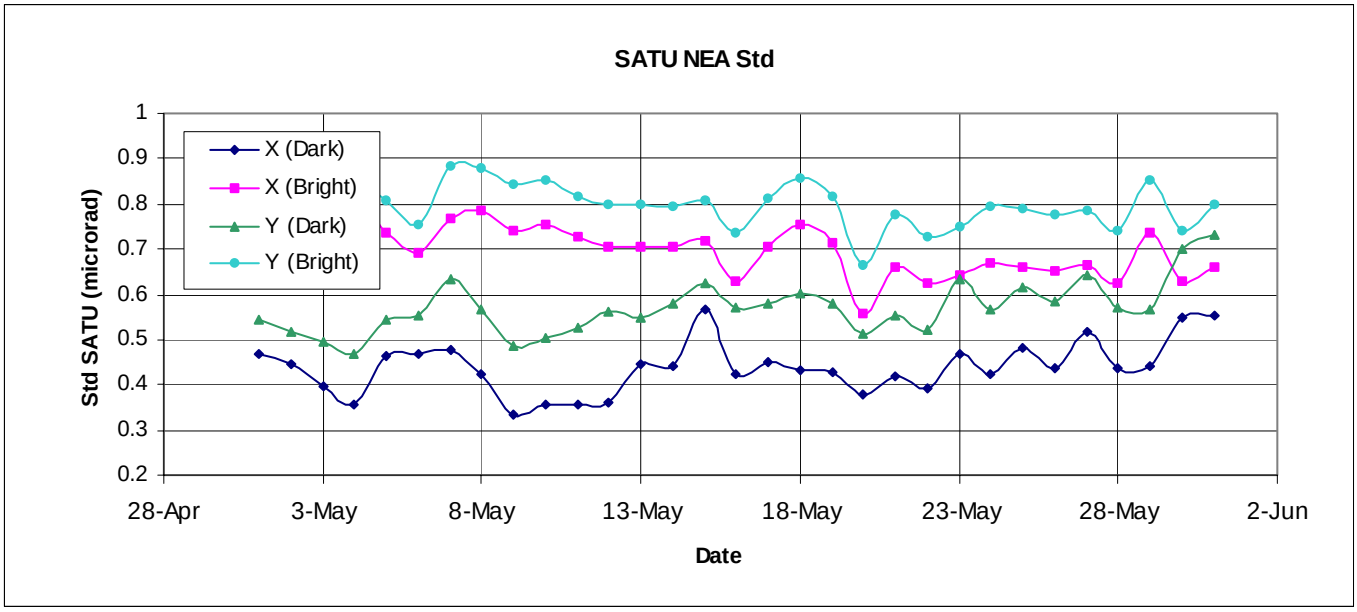

Figure 4.5-1: Average value per day of SATU NEA std above 105 km

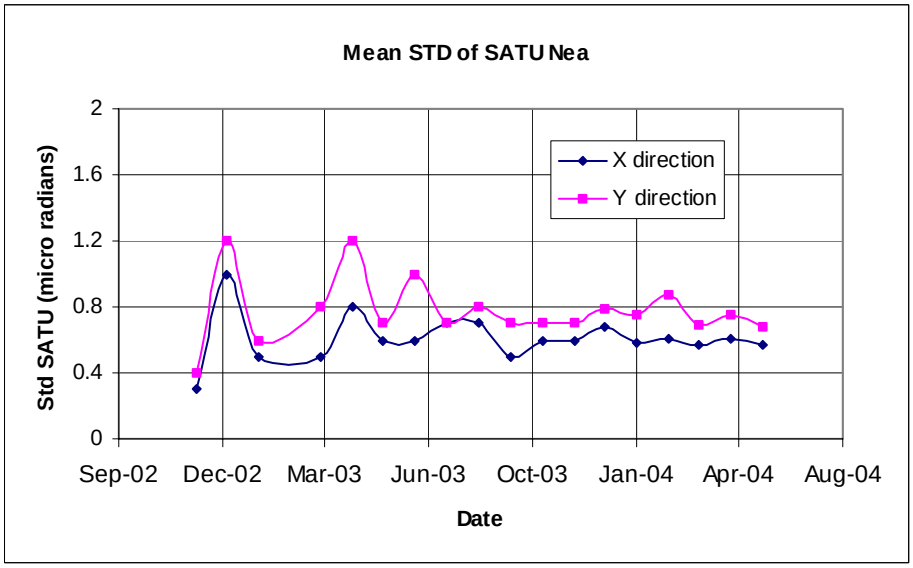

Figure 4.5-2: Average value per month of SATU NEA std above 105 km

4.5.2 TRACKING LOSS INFORMATION

This verification consists of the monitoring of the tangent altitude at which the star is lost. It is an indicator of the pointing performance although it is to be considered that star tracking is also lost due to the presence of clouds and hence not only due to deficiencies in the pointing performance. Therefore, only the detection of any systematic long-term trend is the main purpose of this monitoring. The recent results are presented in fig. 4.5-3 and fig. 4.5-4:

- The dependence of the altitude at which tracking is lost on the magnitude of the star is very small because the tracking is mainly lost due to the refraction and the scintillation that depend on the atmospheric conditions.
- There are no stars lost at a very high altitude in dark (fig. 4.5-3), bright (fig. 4.5-4) or twilight (fig. 4.5-5) limbs.
- Some statistics are given in fig. 4.5-6 calculated for a set of data and not for the whole months. This month the statistics include the twilight limb that has been separated from dark limb. For the moment, no trend is visible in the plot.

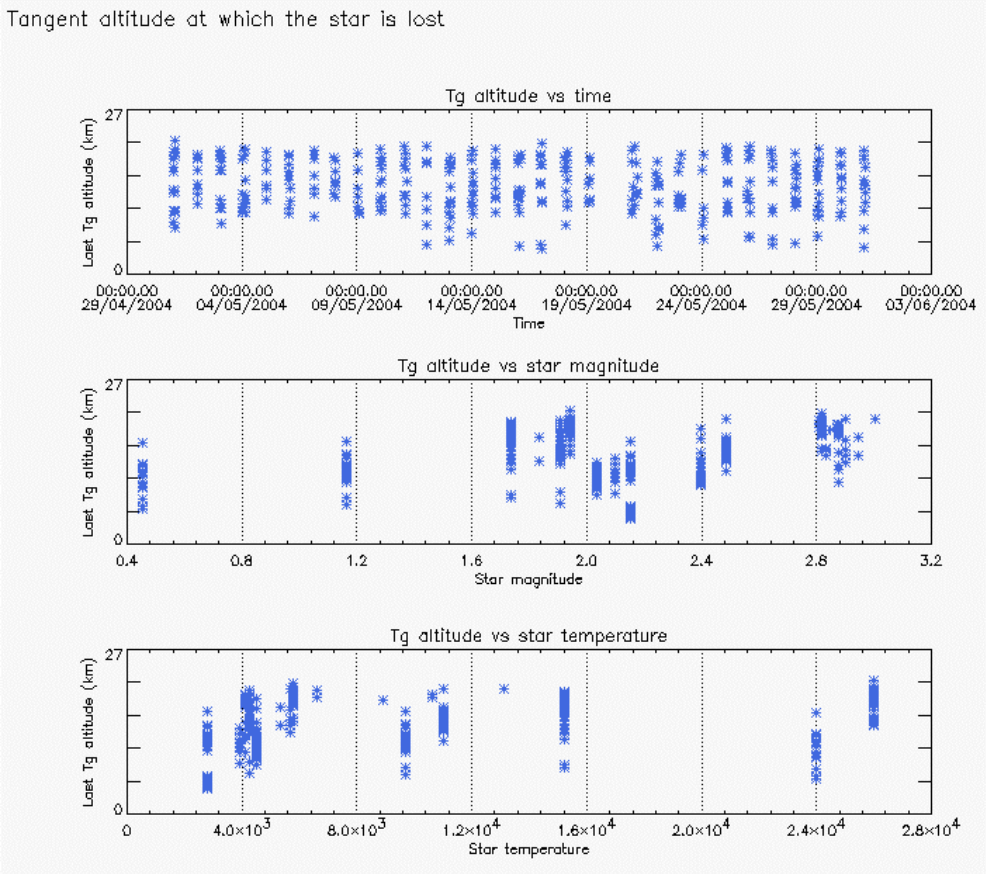

Figure 4.5-3: Last tangent altitude of the occultation (dark limb), point at which the star is lost

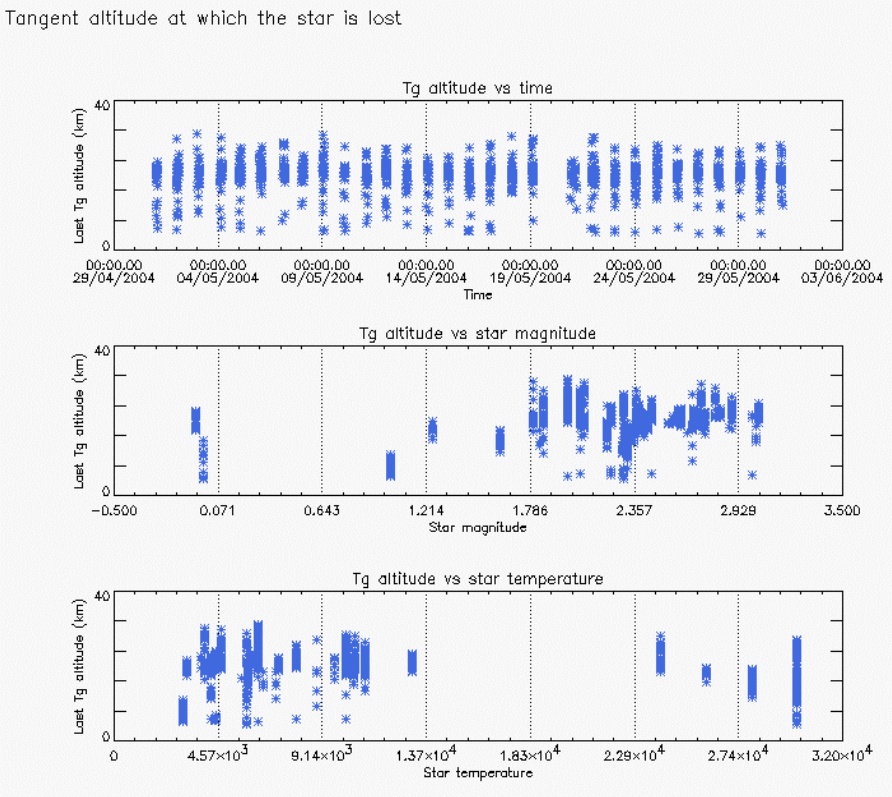

Figure 4.5-4: Last tangent altitude of the occultation (bright limb), point at which the star is lost

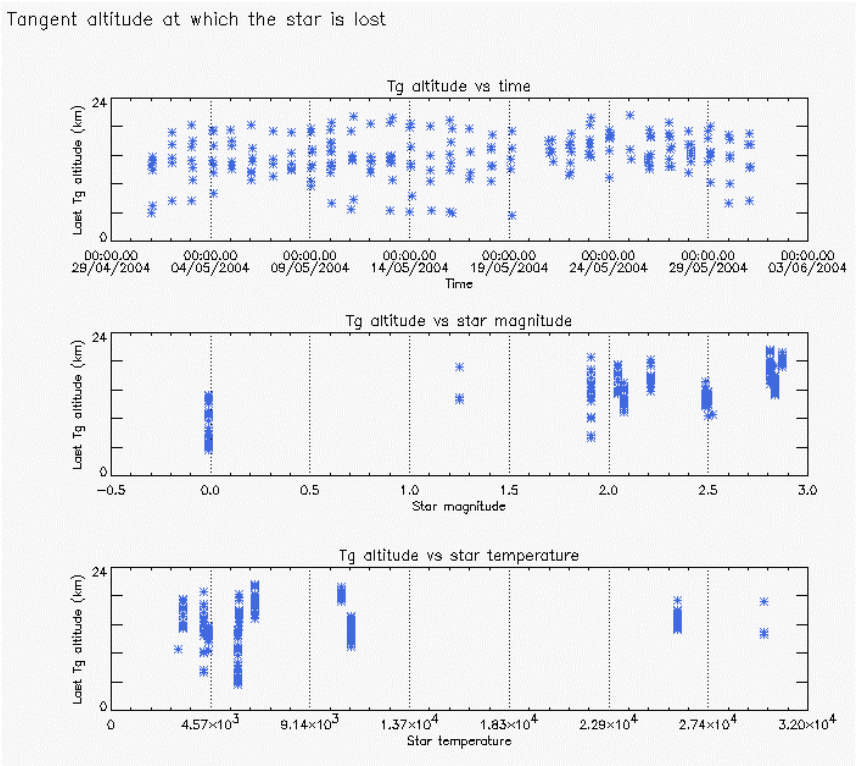

Figure 4.5-5: Last tangent altitude of the occultation (twilight limb), point at which the star is lost

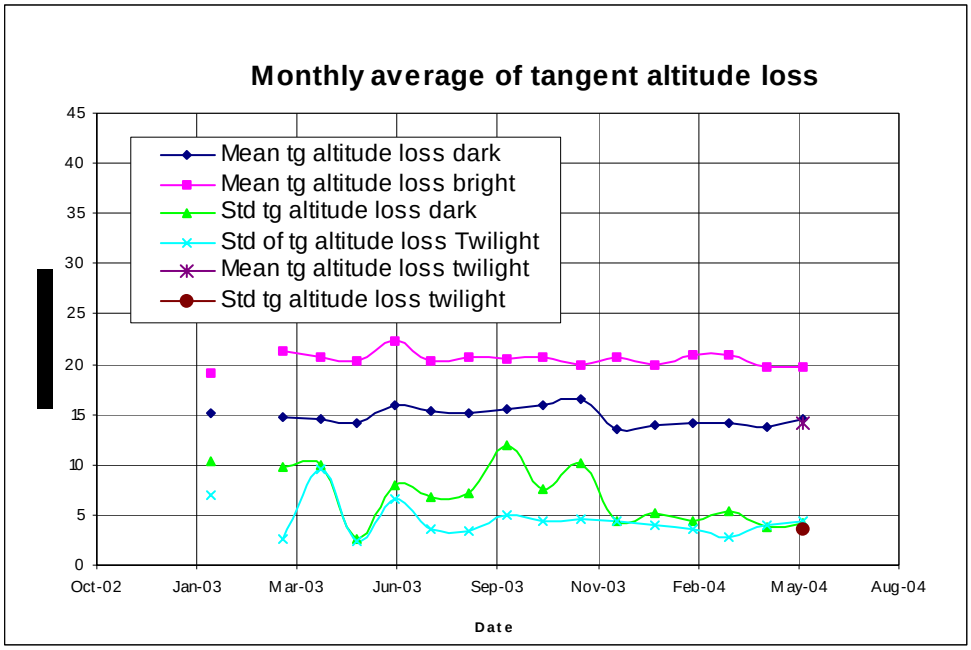

Figure 4.5-6: Monthly mean tangent altitude (and Std) at which the star is lost since January 2003

4.5.3 MOST ILLUMINATED PIXEL (MIP)

The MIP (Most Illuminated Pixel) is the star position on the SATU CCD in detection mode and it is recorded in the housekeeping data. The nominal centre of the SATU is pixel number **145** in elevation and number **205** in azimuth. The detection of the stars should not be far from this centre. As can be seen in fig. 4.5-7 the azimuth is always well within the threshold (table 4.5-1) since September 2002 even if a small variation is present. The elevation MIP has a significant variation (see the *note* below) till 12th December 2003 when a new PSO algorithm was activated in order to reduce the deviations of the ENVISAT platform attitude with respect to the nominal one. The annual amplitude of the MIP displacement is decreased from 18-20 pixels to 8-10 that means an important improvement of the ENVISAT pointing performance. This result confirms that, until now, the algorithm is working as expected. Anyway, the MIP displacement will continue to be carefully monitored during the following months. Fig. 4.5-8 shows the standard deviation of azimuth and elevation that should be within the thresholds of table 4.5-1. The peaks observed mean that one (or more) star/s where detected very far from the SATU centre and, in this case, the star/s is lost during the centering phase (see section 3.2 for stars lost in centering).

Note: A MIP variation onto the SATU CCD of 50 pixels corresponds to a de-pointing of 0.1 degrees

Table 4.5-1: MIP Thresholds

MIP X	**Mean delta Az**	[198 - 210]
	Std delta Az	7
MIP Y	**Mean delta El**	[145 – 154]
	Std delta El	4

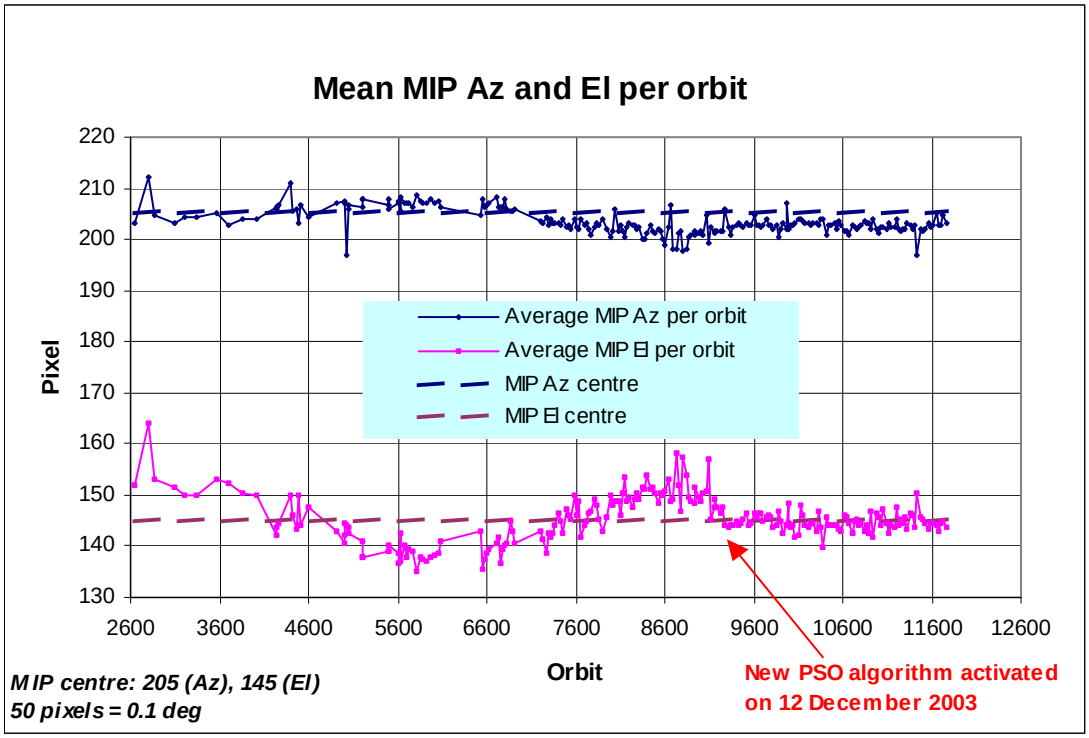

Figure 4.5-7: Mean values of MIP for some orbits since 1st September 2002 (see table 4.5-1)

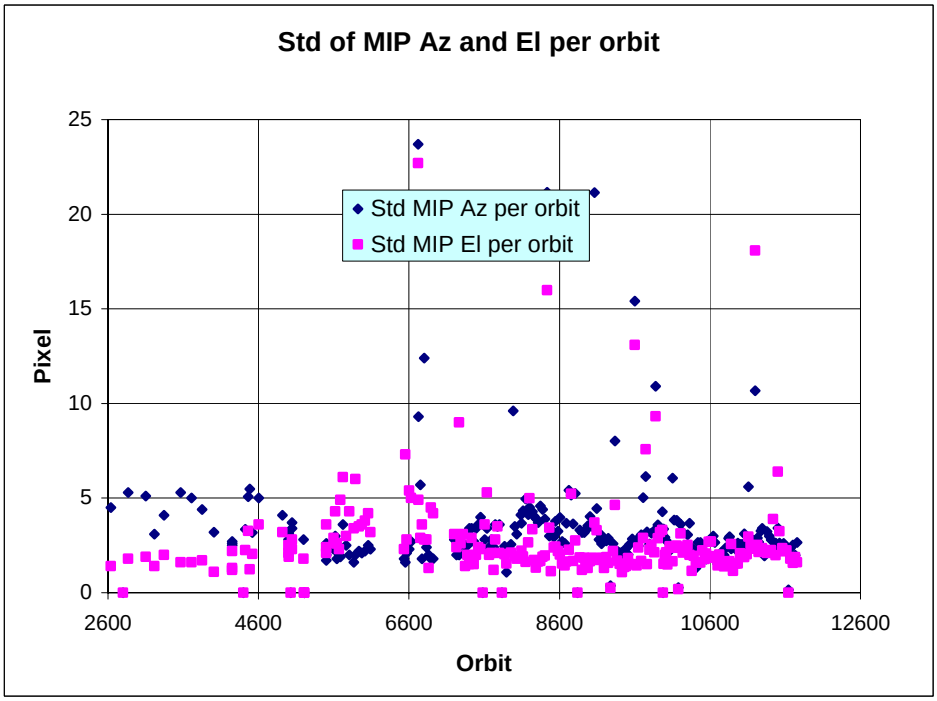

Figure 4.5-8: Standard deviation of MIP Azimuth and Elevation for some orbits since 1st September 2002 until end of reporting period (see table 4.5-1)

5 LEVEL 1 PRODUCT QUALITY MONITORING

5.1 Processor Configuration

5.1.1 VERSION

About 13% of GOM_TRA_1P products have been received in the PCF for routine quality control and long term trend quality monitoring. The current level 1-processor software version for the operational ground segment is GOMOS/4.02 (see table 5.1-1). The product specification is PO-RS-MDA-GS2009_10_3H. This processor has been cleared for initial level 1 data release, with a disclaimer for known artefacts that are currently being resolved and will be implemented in the next release (http://envisat.esa.int/dataproducts/availability).

Cal/Val teams are supplied with selected data sets generated by the prototype processor GOPR 6.0a. See table 5.1-2 for prototype level 1b versions and modifications.

Table 5.1-1: PDS level 1b product version and main modifications implemented

Date	Version	Description of changes
23-MAR-2004	Level 1b version 4.02 at PDHS-E and PDHS-K	Algorithm baseline level 1b DPM 6.0 • Adding a new calibration parameters (these values are hard coded at the moment) • Removal of redundancy chain from code • Modifications in the processing to apply new configuration and calibration parameter • New algorithm to determine between dark, twilight and bright limb and to handle data accordingly • Added handling of source packages with invalid packet header • Added enumerations for all configuration flags • See ref. [2] for more details
31-MAY-2003	Level 1b version 4.00 at PDHS-E and PDHS-K	Algorithm baseline level 1b DPM 5.4: • Modulation correction step added after the cosmic rays detection processing • Inversion of the non-linearity and offset corrections • Modification of the computation of the estimated background signal measured by the photometers: use the spectrometer radiometric sensitivity curve and the photometer transfer function. • Use of the dark charge map at orbit level computed from the DSA (dark sky area) if any in the level 0 product • Implementation of a new unfolding algorithm for the photometer samples • See ref. [2] for more details
21-NOV-2002	Level 1b version 3.61 at PDHS-E and PDHS-K	Algorithm baseline DPM 5.3: • Review of some default values • New definition of one PCD flag (atmosphere) • Temporal interpolation of ECMWF data • See ref. [2] for more details

Table 5.1-2: GOPR level 1b product version and main modifications implemented

Date	Version	Description of changes
17-MAR-2004	GOPR 6.0a	• Provide SFA and SATU angles in degrees • Elevation angle dependency of the reflectivity LUT added in the algorithms • Ratio upper/star signal added (FLAGUC) • Add Dark Charge used for dark charge correction (per band) • Flag for illumination condition (PCDillum) • Minimum sample value for which the cosmic rays detection processing is applied (Crmin) is a function of gain index • Logic for computation of the flags attached to the reference star spectrum (Flref) modified • Add the computation of the sun direction in the inertial geocentric frame to be written in the level 1b and limb products. • Spectrometer effective sampling time added (To be completed)
25-JUL-2003	GOPR 5.4f	• The demodulation process is applied only in full dark limb and twilight limb conditions.
17-JUL-2003	GOPR 5.4e	• Sun zenith angle is computed in the geolocation process. The occultation is now classified into (0) full dark limb condition, (1) bright limb condition and (2) twilight limb condition. • No background correction applied in full dark limb condition. The location of the image of the star spectrum on the CCD array is no more aligned with the CCD lines.
02-JUL2003	GOPR 5.4d	• The maximum number of measurements is set to 509 (instead of 510) in the GOPR prototype.
17-MAR-2003	GOPR 5.4c	• Modification of the CAL ADFs (update of the limb radiometric LUT). The products are affected only if the limb spectra are converted into physical units • Modifications to allow compatibility with ACRI computational cluster (no modifications of the results) • Modification of the logic to handle dark charge map refresh at orbit level (DSA data is now directly processed by the level 1b processor if available in the level 0 product). No impact on the results
21-FEB-2003	GOPR 5.4b	• DC map values are rounded when written in the level 1b product • Modification of the CAL ADFs (update of the wavelength assignment of SPB1 and SPB2) • Modify the computation of flag_mod in the modulation correction routine
17-JAN-2003	GOPR 5.4a	• use the start and stop dates of the occultation when calling the CFI interpol instead of start and stop dates of the level 0 product • modify the ECMWF filename information in the SPH of the level 1b and limb products

5.1.2 AUXILIARY DATA FILES (ADF)

The ADF's files in tables 5.1-3, 5.1-4, 5.1-5, 5.1-6 and 5.1-7 have been disseminated to the PDS during the whole mission. For every type of file, the validity runs from the start validity time until the start validity time of the following one, but if an ADF file has been disseminated after the start validity time, it is obvious that it will be used by the PDS only after the dissemination time (this happens the majority of the times). As the other ADF's, the calibration auxiliary file (GOM_CAL_AX) has been updated several times in the past (table 5.1-7) but the difference is that now it is updated in a weekly basis with only new

DC maps, and that is why the files used in May are reported in a separate table (table 5.1-8) that will changed from month to month. On 18th and 26th May new calibration ADF's were disseminated with updated DC maps of orbits 11561 and 11689 respectively (table 5.1-8). Note that the files outlined in yellow are the set of auxiliary files used during the reporting month.

Table 5.1-3: Table of historic GOM_PR1_AX files used by PDS for level 1b products generation

Used by PDS for Level 1b products generation in period	GOM_PR1_AX (GOMOS processing level 1b configuration file)
01-MAR-2002 → 29-MAR-2002	GOM_PR1_AXVIEC20020121_165314_20020101_000000_20200101_000000 • Pre-launch configuration
30-MAR-2002 → 14-NOV-2002	GOM_PR1_AXVIEC20020329_115921_20020324_200000_20100101_000000 • Changed num_grid_upper, thr_conv and max_iter in the atmospheric GADS
Not used	GOM_PR1_AXVIEC20020729_083756_20020301_000000_20100101_000000 • Cosmic Ray mode + threshold • DC correction based on maps • Non-linearity correction disabled
Not used	GOM_PR1_AXVIEC20021112_170331_20020301_000000_20100101_000000 • Central background estimation by linear interpolation + associated thresholds
15-NOV-2002 → 26-MAR-2003	GOM_PR1_AXVIEC20021114_153119_20020324_000000_20100101_000000 • Same content as GOM_PR1_AXVIEC20021112_170331_20020301_000000_20100101_000000 but validity start updated so as to supersede according to the PDS file selection rules GOM_PR1_AXVIEC20020329_115921_20020324_200000_20100101_000000
27-MAR-2003 → 19-MAR-2004	GOM_PR1_AXVIEC20030326_085805_20020324_200000_20100101_000000 • Same content as GOM_PR1_AXVIEC20021112_170331_20020301_000000_20100101_000000 but validity start updated so as to supersede according to the PDS file selection rules GOM_PR1_AXVIEC20020329_115921_20020324_200000_20100101_000000
20-MAR-2004 → 22-MAR-2004	GOM_PR1_AXVIEC20040319_134932_20020324_200000_20100101_000000 • Ray tracing parameter changed: convergence criteria set to 0.1 microrad
23-MAR-2004 → 01-APR-2004 *Notes*: • This file was constructed from GOM_PR1_AXVIEC20030326_085805_20020324_200000_20100101_000000 (so without the ray tracing parameter changed) • This file was used by the GOMOS/4.02 processors before the IECF dissemination. The dissemination was done on 25th March 2004	GOM_PR1_AXVIEC20040316_144850_20020324_200000_20100101_000000 GOM_PR1 ADF for version GOMOS/4.02, changes: • The central band estimation mode • Atmosphere thickness • Altitude discretisation

02-APR-2004	GOM_PR1_AXVIEC20040401_083133_20020324_200000_20100101_000000 • Ray tracing parameter changed: convergence criteria set to 0.1 microrad

Table 5.1-4: Table of historic GOM_INS_AX files used by PDS for level 1b products generation

Used by PDS for Level 1b products generation in period	GOM_INS_AX (GOMOS instrument characteristics file)
01-MAR-2002 → 29-JUL-2002	GOM_INS_AXVIEC20020121_165107_20020101_000000_20200101_000000 • Pre-launch configuration
30-JUL-2002 → 12-NOV-2002	GOM_INS_AXVIEC20020729_083625_20020301_000000_20100101_000000 • Factors for the conversion of the SFA angles from SFM axes to GOMOS axes
13-NOV-2002 → 16-JUL-2003	GOM_INS_AXVIEC20021112_170146_20020301_000000_20100101_000000 • No more invalid spectral range
Not used	GOM_INS_AXVIEC20030716_080112_20030711_120000_20100101_000000 • New value for SFM elevation zero offset for redundant chain: 10004
17-JUL-2003	GOM_INS_AXVIEC20030716_105425_20030716_120000_20100101_000000 • Bias induct azimuth redundant value set to -0.0084 rad (-0.4813 deg)

Table 5.1-5: Table of historic GOM_CAT_AX files used by PDS for level 1b products generation

Used by PDS for Level 1b products generation in period	GOM_CAT_AX (GOMOS Stat Catalogue file)
01-MAR-2002	GOM_CAT_AXVIEC20020121_161009_20020101_000000_20200101_000000 • Pre-launch configuration

Table 5.1-6: Table of historic GOM_STS_AX files used by PDS for level 1b products generation

Used by PDS for Level 1b products generation in period	GOM_STS_AX (GOMOS Star Spectra file)
01-MAR-2002	GOM_STS_AXVIEC20020121_165822_20020101_000000_20200101_000000 • Pre-launch configuration

Table 5.1-7: Table of historic GOM_CAL_AX files used by PDS for level 1b products generation

Used by PDS for Level 1b products generation in period	GOM_CAL_AX (GOMOS Calibration file)
01-MAR-2002 → 29-JUL-2002	GOM_CAL_AXVIEC20020121_164808_20020101_000000_20200101_000000 • Pre-launch configuration
Not used	GOM_CAL_AXVIEC20020121_142519_20020101_000000_20200101_000000 • Pre-launch configuration
30-JUL-2002 → 12-NOV-2002	GOM_CAL_AXVIEC20020729_082426_20020717_193500_20100101_000000 • Band setting information • Wavelength assignment • Spectral dispersion LUT • ADC offset for Spectrometers

	• PRNU maps • Thermistor coding LUT • DC maps
Not used	GOM_CAL_AXVIEC20021112_165603_20020914_000000_20100101_000000 • Band setting information • DC maps • PRNU maps • Wavelength assignment • Spectral dispersion LUT • Radiometric sensitivity LUT (star and limb) • SP-FP intercalibration LUT • Vignetting LUT • Reflectivity LUT • ADC offset
13-NOV-2002 → 30-JAN-2003	GOM_CAL_AXVIEC20021112_165948_20021019_000000_20100101_000000 • Only DC maps updated
31-JAN-2003 → 11-APR-2003	GOM_CAL_AXVIEC20030130_133032_20030101_000000_20100101_000000 • Only DC maps updated (using DSA of orbit 04541)
12-APR-2003 → 02-JUN-2003	GOM_CAL_AXVIEC20030411_065739_20030407_000000_20100101_000000 • Modification of the radiometric sensitivity curve for the limb spectra. Note that the modification of this LUT has no impact on the GOMOS processing. The LUT is just copied into the level 1b limb product for user conversion purpose. • Updated DC map only (using DSA of orbit 05762).
03-JUN-2003: from this date onwards, mainly updates to DC maps are done. Every month, the table of new GOM_CAL files with only DC maps updated is provided (table 5.1-8). Eventual changes to this file not corresponding only to DC maps updates will be reported in this table.	GOM_CAL_AXVIEC20030602_094748_20030531_000000_20100101_000000 • Updated DC maps only (using DSA of orbit 06530)
13-FEB-2004 → 23-FEB-2004	GOM_CAL_AXVIEC20040212_103916_20040209_000000_20100101_000000 • Update of the reflectivity LUT • Updated DC maps (Orbit 10194, date 11-FEB-2004)

Table 5.1-8: Calibration ADF for reporting month. These files are updated (only with DC maps) in a 8-10 days basis

Used by PDS for Level 1b products generation in period	GOM_CAL_AX (GOMOS Calibration file)
19-MAY-2004 → 26-MAY-2004	GOM_CAL_AXVIEC20040518_131933_20040515_000000_20100101_000000 (Orbit 11561, date 16-MAY-2004)
27-MAY-2004	GOM_CAL_AXVIEC20040526_125214_20040524_000000_20100101_000000 (Orbit 11689, date 24-MAY-2004)

5.2 Quality Flags Monitoring

In this section it is monitored some Product Quality information stored in level 1b products that did not have a fatal error (MPH error flag not set). The products with fatal errors were around 1.7% of the products received during May for the quality monitoring.

On the one hand, for every product we have information of the **number of measurements** where a given problem was detected (i.e. number of invalid measurements, number of measurements containing saturated samples, number of measurements with demodulation flag set…). On the other hand, there are **flags** that indicate problems within the product (i.e. flag set to one if the reference spectrum was computed from DB, flag set to zero if SATU data were not used…).

For the information on the number of measurements a plot of percentages with respect to time is provided in fig. 5.2-1. Part of this information, the most relevant one, is also plotted in a world map as a function of ENVISAT position: % of cosmic ray hits per profile, % of datation errors per profile, % of star falling outside the central band per profile and % of saturation errors per profile (fig.5-2.2).

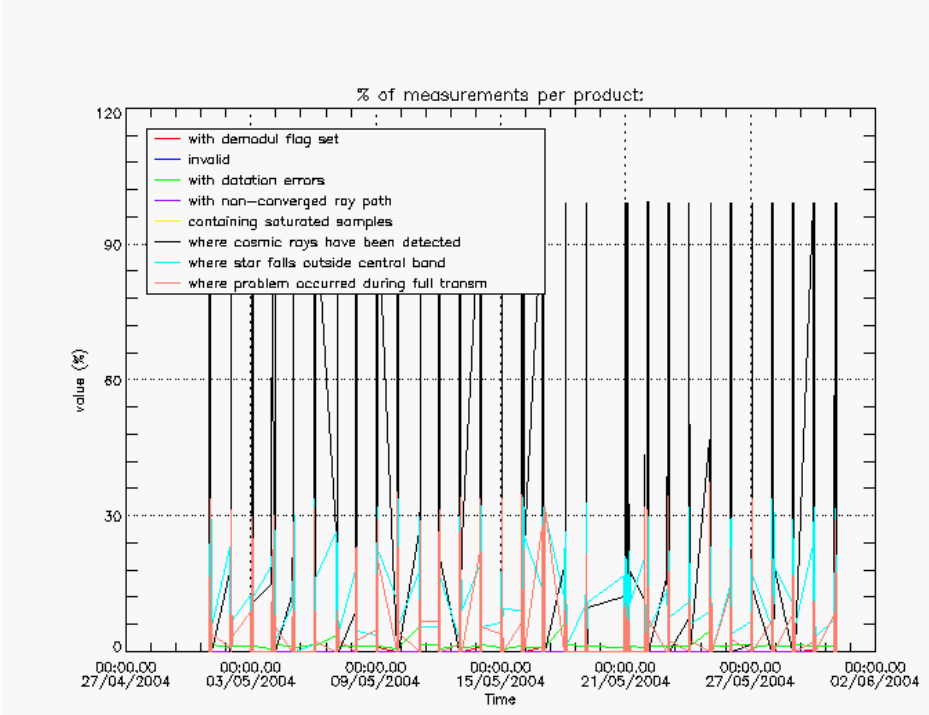

Figure 5.2-1: Level 1b product quality monitoring with respect to time

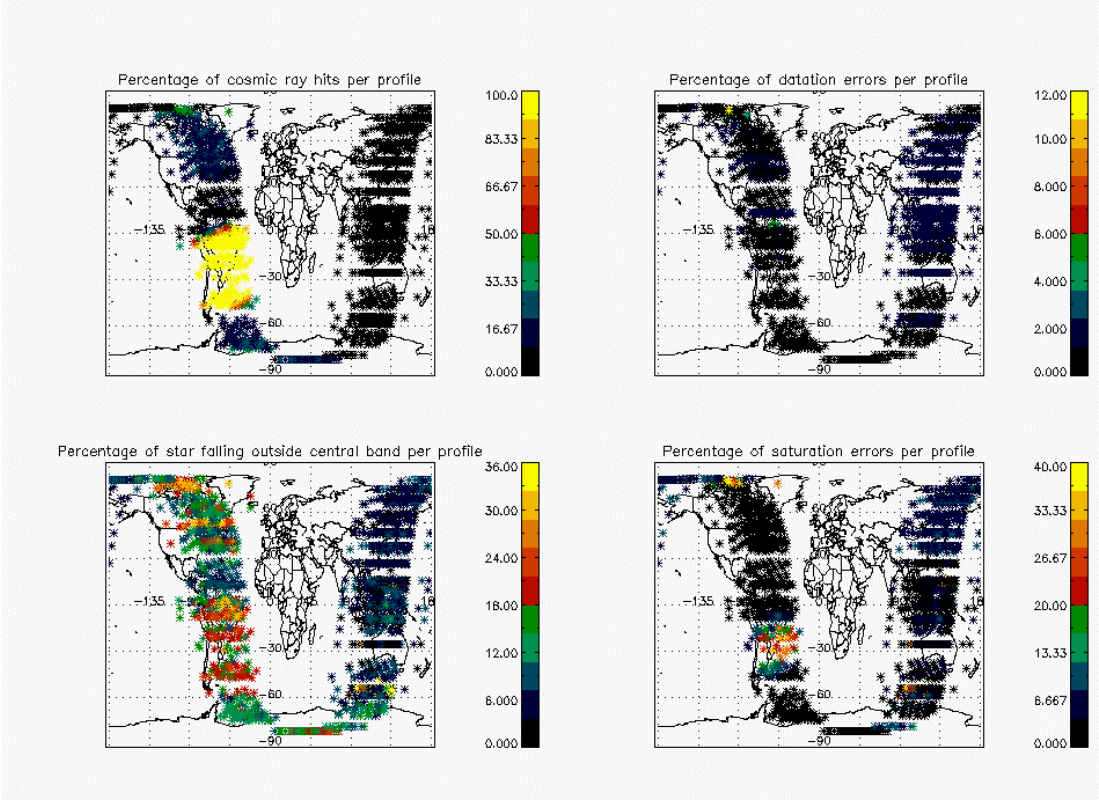

Figure 5.2-2: Level 1b product quality monitoring with respect to geolocation of ENVISAT

It can be seen from fig. 5.2-1 that the cosmic rays hits occurred several times for the 95% of the measurements of the products. Looking at fig. 5.2-2 it can be clearly observed that this high percentage occurred when the satellite crossed the South Atlantic Anomaly (SAA) zone. Also the percentage of saturation errors per profile increased in this zone. Another observation from fig. 5.2-1 is that, for many products, the 25 % of the measurements have the star signal falling outside the central band. In fig. 5.2-2 it is observed that this percentage occurred mainly during the ascending part of the orbit while in the descending part the percentage is around 10 %. The other values (% of invalid measurements per product, % of measurements per product with datation errors…) are quite low.

The flag information is given in table 5.2-1. It is reported also the percentage of the products that have at least one measurement with demodulation flag set.

Table 5.2-1: Percentage of products during the reporting period with:

At least one measurement with demodulation flag set:	17.1400 %
Reference spectrum computed from DB:	0.00000 %
Reference spectrum with small number of measurements:	0.00000 %
SATU data not used:	0.00000 %

5.3 Spectral Performance

No spectral calibration has been performed in May. The last calibration was done during April with results that reach the warning value.

The values reported (table 5.3-1) are, for every star ID (1, 2, 4, 9, 18, 25), the wavelength of the first useful pixel of SPA2. This value is calculated by addition to the actual wavelength assignment, the spectral shift for which a maximum correlation has been found between the reference spectrum and the one of the occultation.

During the last wavelength calibration analysis performed using several occultations, the spectral shifts are 0.09 for star id number 1, 0.078 for star id number 2 and 0.072 for star id number 18 (see table 5.3-1). These shifts are greater than 0.07 (warning value) and QWG investigation has been initiated on March.

The star number 4 is left in table 5.3-1 even if the values of the wavelength are very different from the nominal one. It should be just kept in mind that the values of the shift should be always of the same order (~0.4) but this star will not be used for calibration purposes.

Table 5.3-1: Wavelength assignment calculated for several occultations since November 2002

Star ID / Level 0 date	1	2	4	9	18	25
20021112_062935	Occ.30: 690.455750	Occ.26: 690.458740		Occ.28: 690.492981		
20021219_102754		Occ.33: 690.468140	Occ.26: 690.875122			
20030101_151630	Occ.3: 690.445068	Occ.37: 690.466003	Occ.30: 690.878540			
20030110_121504		Occ.32: 690.465088	Occ.25: 690.882385			
20030201_090221						Occ.21: 690.492981
20030415_123156			Occ.29: 690.959534		Occ.20: 690.552002	Occ.28: 690.492981
20030419_170041			Occ.29: 690.957520		Occ.23: 690.555420	
20030428_072600					Occ.19: 690.553645	Occ.28: 690. 492981
20030717_053233				Occ. 22: 690.473816	Occ. 26: 690.446594	
20040123_091615	Occ.1: 690.400513 Occ.40: 690.401550	Occ.35: 690.415161	Occ.27: 690.852478			
20040222_065917			Occ.25: 690. 850830			Occ.21: 690. 492981
20040128_163559	Occ.3: 690.399414					Occ.23: 690. 492981

5.4 Radiometric Performance

5.4.1 RADIOMETRIC SENSITIVITY

The monitoring performed consists in the calculation of the radiometric sensitivity of each CCD by computing the ratio between parts of the reference spectrum using specific stars. The parts of spectrum used are:

- UV: 250–300 nm
- Yellow: 500–550 nm
- Red: 640–690 nm
- Ir1: 761-770 nm
- Ir2: 935-944 nm

For the spectrometers the ratios are with respect to the 'yellow' spectral range. For the photometers, the ratio is calculated dividing the mean photometer signal above the atmosphere (115 km) by the 'yellow' spectral range (for PH1) or by the 'red' spectral range (for PH2).

The variation of the normalized ratio should be within a given threshold actually set to 10% (see table 5.4-1 that corresponds to fig. 5.4-1). For every star, this variation is calculated as the difference between the maximum (or minimum) ratio, and the mean over the 15 first values (if there are not 15 values computed yet, all values are used).

Table 5.4-1: Variation of RS for the different ratios (corresponds to fig.5.4-1). Should be less than 10%

Star Id	% Variation of UV ratio	% Variation of Red ratio	% Variation of IR1 ratio	% Variation of IR2 ratio	% Variation of Ph1 ratio	% Variation of Ph2 ratio
1	0.543863	0.207967	0.401701	0.193903	8.55029	30.1656
2	0.158766	0.259793	0.625175	0.216532	4.52068	6.07233
4	0.106818	0.678080	1.17073	1.16053	8.08780	23.5227
9	3.26306	0.312340	0.364793	0.233455	4.79555	9.05862
18	0.522947	0.681692	0.844914	0.852089	14.7885	299.989
25	10.1693	0.699922	0.654513	1.12662	15.9214	78.6219

Values outside the warning threshold set to 10% are observed for the photometers, and investigations were performed by the QWG. An inaccurate reflectivity correction LUT was suspected to be the cause of the increase but a new one is in use since 12th February 2004 and as it can be seen in fig. 5.4-2 and in table 5.4-2, the ratios for star number 4 and 25 are already outside the threshold. New investigations have shown that the increase could be related to the fact that the occultation illumination condition starts to include twilight/straylight. To verify this, the computation of the ratios will be performed using only occultations in full dark conditions and compared to the previous results.

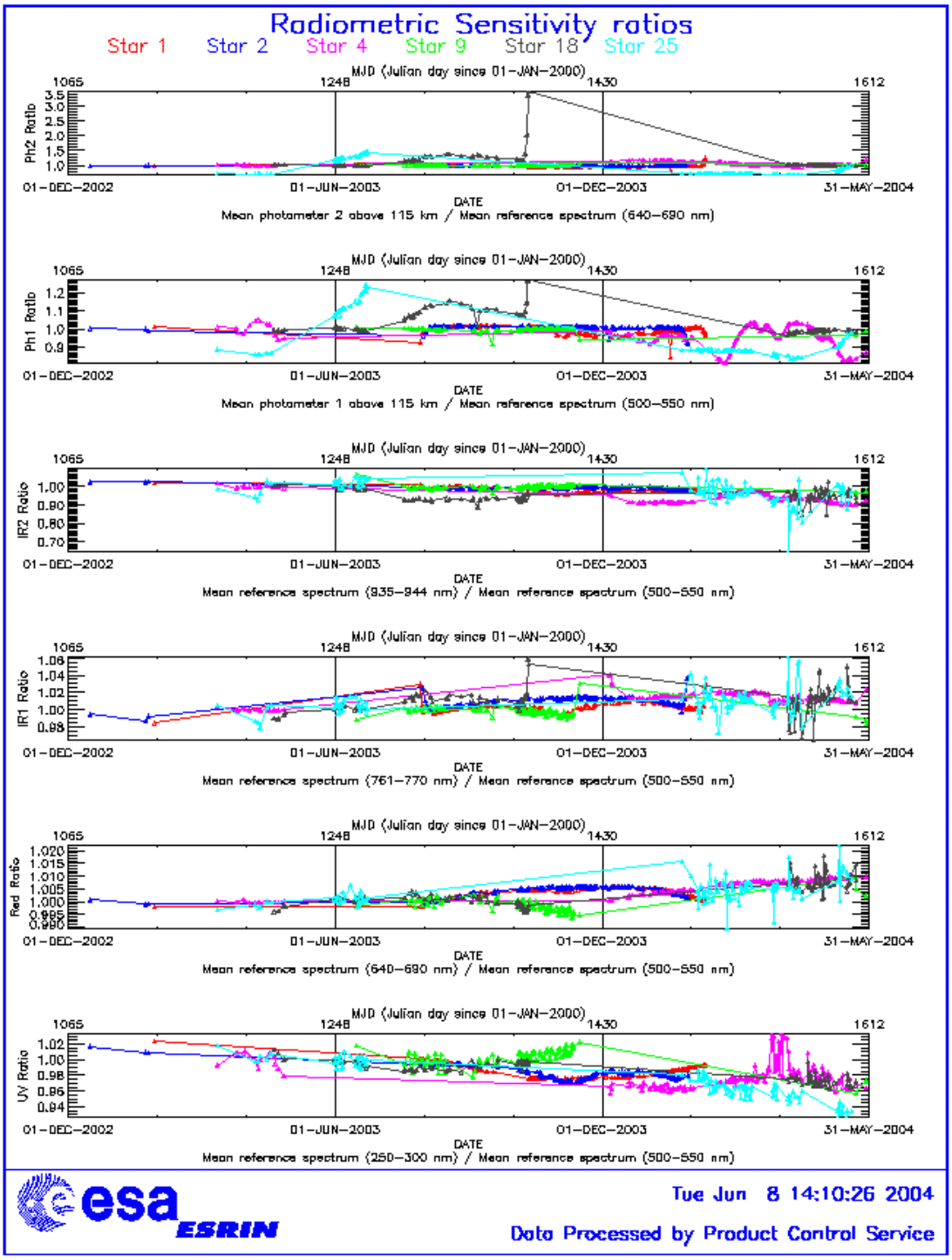

Figure 5.4-1: Radiometric sensitivity ratios since December 2002

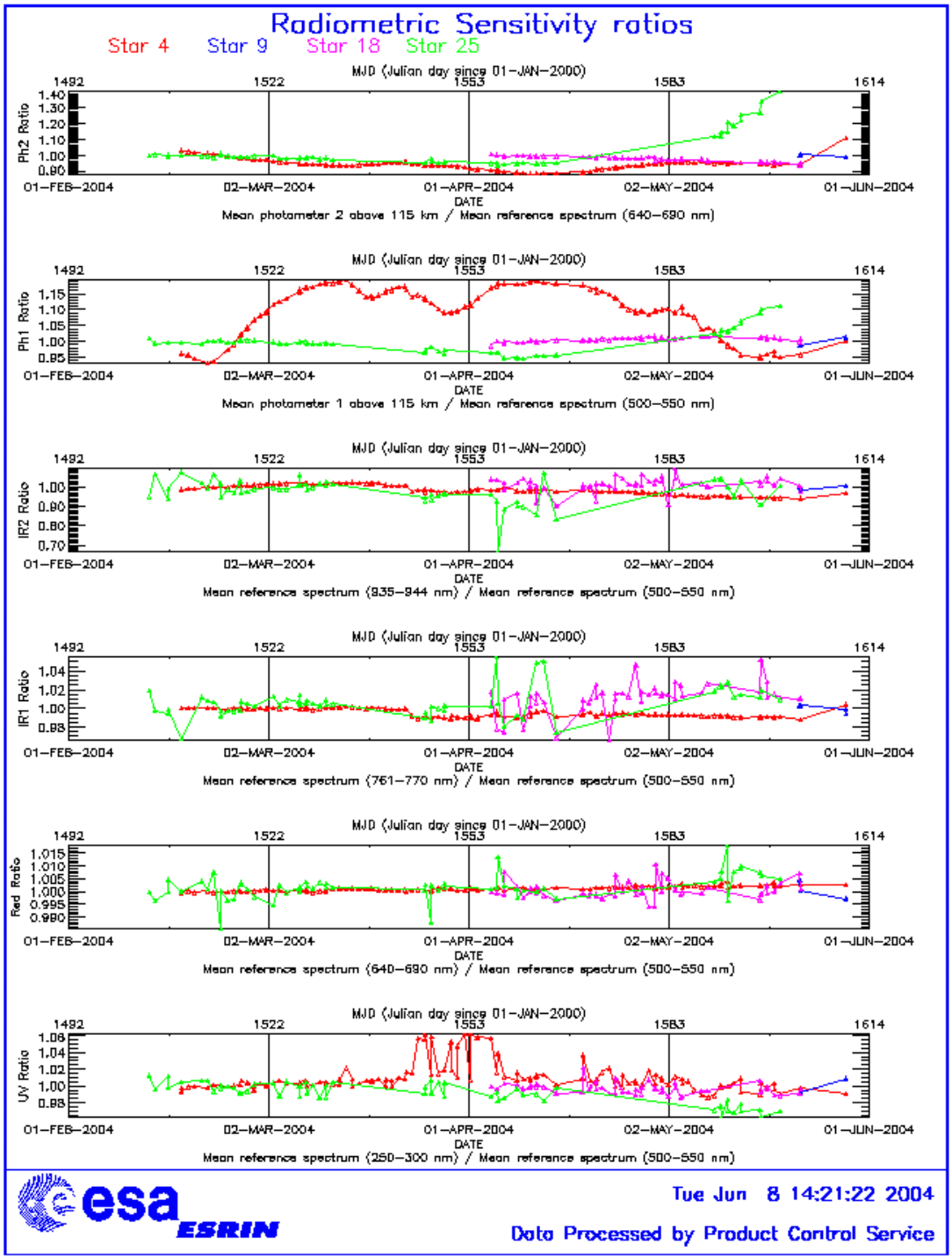

Figure 5.4-2: Radiometric sensitivity ratios since the change in the Reflectivity LUT

Table 5.4-2: Variation of RS for the different ratios since the change in reflectivity LUT (corresponds to fig. 5.4-2)

Star Id	% Variation of UV ratio	% Variation of Red ratio	% Variation of IR1 ratio	% Variation of IR2 ratio	% Variation of Ph1 ratio	% Variation of Ph2 ratio
4	0.151019	0.243592	0.356695	0.654567	7.21849	15.3352
9	0.668299	0.155655	0.0616506	0.0514399	0.738120	1.36600
18	0.304873	0.404969	0.744398	0.510854	0.919706	6.90272
25	4.97413	0.575715	0.593019	1.03292	6.42962	48.2720

5.4.2 PIXEL RESPONSE NON UNIFORMITY

No new PRNU calibration has been done during the reporting month. During May 2003 a new PRNU calibration has been performed and processed into an update of the PRNU maps for the SPB1 and SPB2 that have been included in the auxiliary file GOM_CAL disseminated at the end of June 2003.

5.5 Other Calibration Results

Future reports will address other calibration results, when available.

6 LEVEL 2 PRODUCT QUALITY MONITORING

6.1 Processor Configuration

6.1.1 VERSION

No level 2 products from the operational ground segment have been disseminated during May to the users. About 95% of GOM_NL__2P products have been received in the PCF for routine quality control and long term trend monitoring. The current level 2-processor software version for the operational ground segment is GOMOS/4.02 (see table 6.1-1). The product specification is PO-RS-MDA-GS2009_10_3H. The improvements defined at the first Validation Workshop have been implemented into the prototype processor GOPR 6.0a (see table 6.1-2), before implementation into the operational one. In the mean time, Cal/Val teams are supplied with selected data sets generated by this prototype processor.

Table 6.1-1: PDS level 2 product version and main modifications implemented

Date	Version	Description of changes
23-MAR-2003	Level 2 version 4.02 at PDHS-E and PDHS-K	Algorithm baseline level 2 DPM 5.5: Section 3 • Add references to technical notes on Tikhonov regularization • Change High level breakdown of modules: SMO/PFG

		• Change parameter: NFS in l2 ADF • Change parameter σ_G in l2 ADF (Table 3.4.1.1-II) • Change content of Level 2/res products - GAP • Change time sampling discretisation • Add covariance matrix explanation Section 5 • Replace SMO by PFG VER-1/2: Depending on NFS, Apply either a Gaussian filter or a Tikhonov regularization to the vertical inversion matrix • Unit conversion applied on kernel matrix • Suppress VER-3 Section 6 • GOMOS Atmospheric Profile (GAP): not used in this version • Time sampling in equation (6.5.3.7-73) • See ref. [3] for more details
31-MAY-2003	Level 2 version 4.00 at PDHS-E and PDHS-K	Algorithm baseline level 2 DPM 5.4: • Revision of some default values • Add a new parameter • Transmission model computation: suppress tests on valid pixels and species • Apply a Gaussian filter to the vertical inversion matrix • Very low signal values are substituted by threshold value • See ref. [3] for more details
21-NOV-2002	Level 2 version 3.61 at PDHS-E and PDHS-K	Algorithm baseline level 2 DPM 5.3a: • Revision of some default values • Wording of test T11 • Dilution term computation of jend • Covariance computation scaling applied before and after • See ref. [3] for more details

Table 6.1-2: GOPR level 2 product version and main modifications implemented

Date	Version	Description of changes
17-MAR-2004	GOPR 6.0a	• Rename Turbulence MDS into High Resolution Temperature MDS (HRTP) • Add vertical resolution per species in local densities MDS • Add Solar zenith angle at tangent point and at satellite level in geolocation ADS • Add "tangent point density from external model" in geolocation ADS • Suppress contribution of "tangent point density from external model" in "local air density from GOMOS atmospheric profile" in geolocation ADS

		(to be completed)
18-AUG-2003	GOPR 5.4d	• Tikhonov regularisation is implemented
18-MAR-2003	GOPR 5.4b	• Modification to implement the computation of Tmodel for spectrometer B (in version 5.4b, the Tmodel for SPB is still set to 1)
30-JAN-2003	GOPR 5.4a	• Modifications for ACRI internal use only. No impact on level 2 products.

6.1.2 AUXILIARY DATA FILES (ADF)

The ADF's files in table 6.1-3 and 6.1-4 are used by the PDS to process the data from level 1 to level 2. For every type of file, the validity runs from the start validity time until the start validity time of the following one, but if an ADF file has been disseminated after the start validity time, it is obvious that it will be used by the PDS only after the dissemination time (this happens the majority of the times).

Table 6.1-3: Table of historic GOM_PR2_AX files used by PDS for level 2 products generation

Used by PDS for Level 2 products generation in period	GOM_PR2_AX (GOMOS Processing level 2 configuration file)
01-MAR-2002 → 29-JUL-2002	GOM_PR2_AXVIEC20020121_165624_20020101_000000_20200101_000000 • Pre-launch configuration
30-JUL-2002 → 02-SEP-2002	GOM_PR2_AXVIEC20020729_083851_20020301_000000_20100101_000000 • Maximum value of chi2 before a warning flag is raised (set to 5) • Maximum number of iterations for the main loop (set to 1)
03-SEP-2002 → 12-NOV-2003	GOM_PR2_AXVIEC20020902_151029_20020301_000000_20100101_000000 • Maximum value of chi2 before a warning flag is raised (set to 100)
13-NOV-2003 → 22-MAR-2004	GOM_PR2_AXVIEC20021112_170458_20020301_000000_20100101_000000 • Smoothing mode • Hanning filter • Number of iterations • Spectral windows to suppress the O2 absorption in the high spectral range of SPA2
23-MAR-2004 *Note*: this file was used by the GOMOS/4.02 processors before the IECF dissemination. The dissemination was done on 25th March 2004	GOM_PR2_AXVIEC20040316_145613_20020301_000000_20100101_000000 • Pressure at the top of the atmosphere • Number of GOMOS sources data (used in GAP) • Activation flag for GOMOS sources data (GAP) • Smoothing mode (after the spectral inversion) • Atmosphere thickness

Table 6.1-4: Table of historic GOM_CRS_AX files used by PDS for level 2 products generation

Used by PDS for Level 2 products generation in period	GOM_CRS_AX (GOMOS Cross Sections file)
01-MAR-2002 → 08-MAR-2002	GOM_CRS_AXVIEC20020121_164026_20020101_000000_20200101_000000 • Pre-launch configuration
09-MAR-2003 → 29-JUL-2002	GOM_CRS_AXVIEC20020308_185417_20020101_000000_20200101_000000 • Corrected NUM_DSD in MPH - was 14 and is now 19 - and corrected spare DSD format by replacing last spare by carriage returns in file

	GOM_CRS_AXVIEC20020121_164026_20020101_000000_20200101_000000
30-JUL-2002 → 25-MAR-2004	GOM_CRS_AXVIEC20020729_082931_20020301_000000_20100101_000000 • O3 cross-sections summary description (SPA) • NO3 cross-sections summary description • O2 transmissions summary description • H2O transmissions summary description • O3 cross sections (SPA)
26-MAR-2004 *Note*: the file was disseminated on 27 Jan 2004 but could not be used by PDS until version GOMOS/4.02 was in operation	GOM_CRS_AXVIEC20040127_150241_20020301_000000_20100101_000000 • Update of the O2 and H2O transmissions (S.A input) • Extension by continuity of the O3 cross-section for SPB

6.2 Quality Flags Monitoring

In this section it is plotted some information contained in the Quality Summary data set of the level 2 products. In particular, it is depicted the percentage of flagged points per profile for the local species O_3, H_2O, NO_2 and Air. Only products in dark limb conditions and without fatal errors (error flag in the MPH set to "0") are used.

A profile point in a level 2 product is flagged when:

- The local density is less than a given minimum value
- The local density is greater than a given maximum value
- A negative local density was found
- The line density is not valid. And it occurs when:
  - The acquisition from level 1b is not valid
  - There is no acquisition used for reference star spectrum
  - The line density is less than a given minimum value
  - The line density is greater than a given maximum value
  - A negative line density was found

  For species: air, aerosol, O_3, NO_2, NO_3, OClO
  - No convergence after a given number of LMA iterations
  - χ^2 out of LMA is bigger than χ^2
  - Failure of inversion

  For species: O_2, H_2O
  - Spectro B only: no convergence
  - Spectro B only: data not available
  - Spectro B only: covariance not available

Looking at the fig. 6.2-1 the most evident characteristic that can be observed is the high percentage of flagged points per profile for H_2O. Users should not use these data, as their quality is still poor. The percentage of flagged points per profile for O_3 and Air is around 40% whereas for NO_2 it becomes 60%.

The same information is plotted in fig. 6.2-2 as a function of the first tangent point of every profile. In the SAA the percentages of flagged points per profile are slightly higher than in the rest of the world for O_3, NO_2 and Air. It can be seen also that there are latitudinal bands with almost the same color (same

percentages). This means that the percentages of flagged points per profile have a dependence on the stars that have been observed: a given star is always observed at the same latitude but at different longitude.

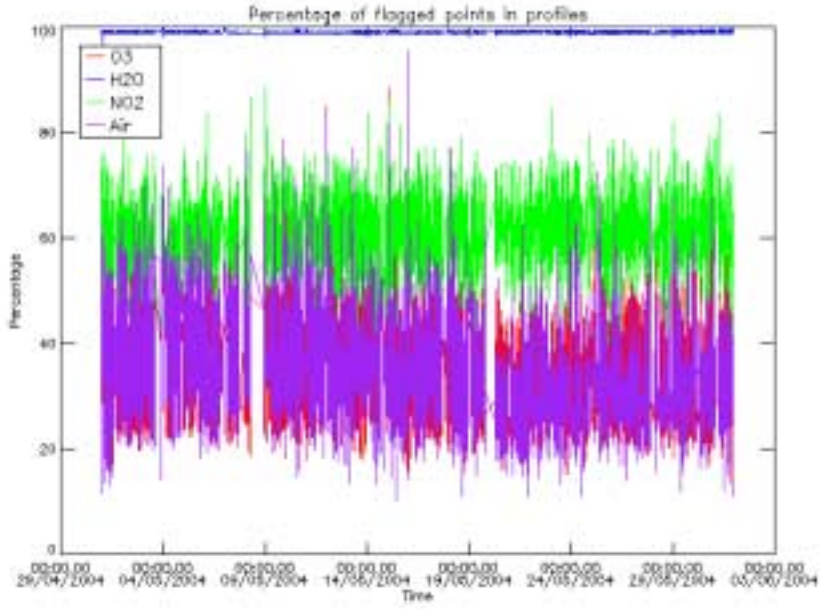

Figure 6.2-1: Percentage of flagged points per profile

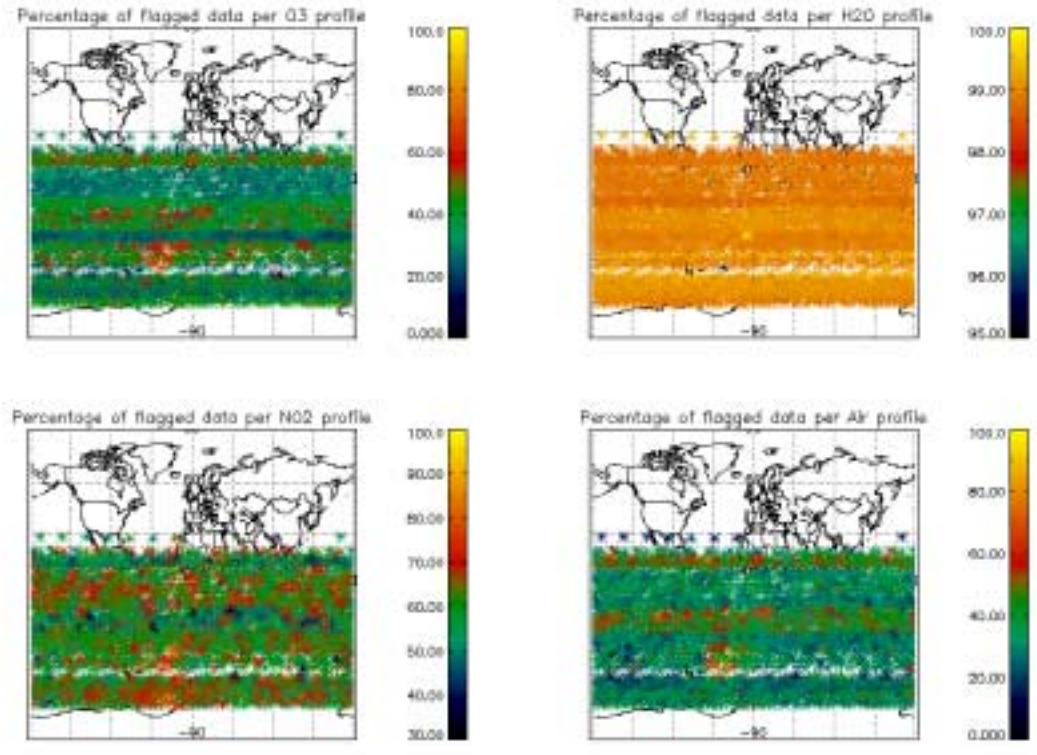

Figure 6.2-2: Percentage of flagged points per profile as a function of the first tangent point of the profile

6.3 Other Level 2 Performance Issues

The plot presented in fig. 6.3-1 is the average of the Ozone values during May in a grid of 0.5 degrees in latitude per 1 km in altitude. Some known characteristics can be seen:

- O_3 concentrations show a decrease with latitude near 40 km altitude. In the lower latitudes O_3 is generated by photolysis of O_2
- In the middle stratosphere (25-30 km) O_3 is strongly influenced by transport effects. Strong meridional and zonal transport is visible in middle and higher latitudes
- The lower stratosphere shows an O_3 increase with latitude. Highest values can be found within the polar regions due to downward transport of rich air masses

However, other characteristics seem not to be realistic as the values below 15 km, where data are not reliable at the moment or some high values at –45 degrees latitude at high altitude (issues currently under investigation).

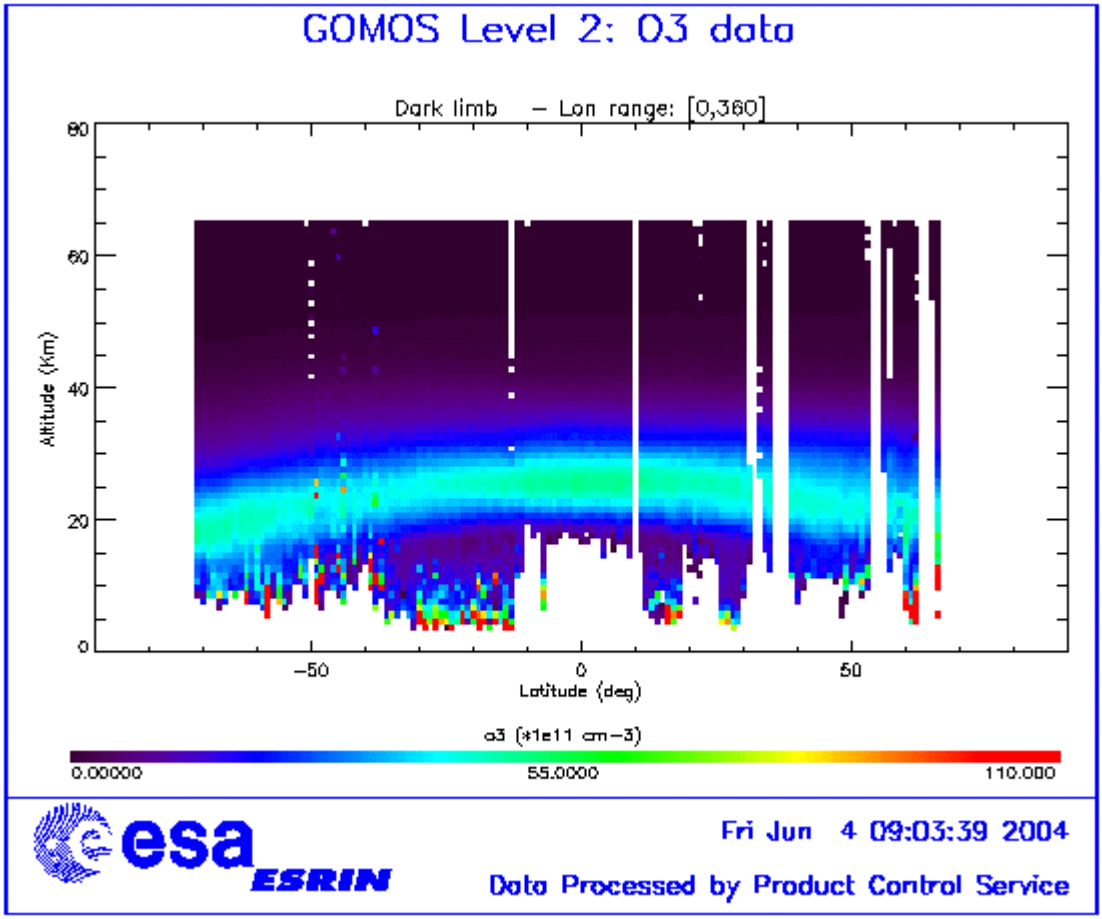

Figure 6.3-1: Average GOMOS O_3 profile during May: average in a grid of 0.5° latitude x 1 km altitude

7 VALIDATION ACTIVITIES AND RESULTS

7.1 Inter-comparison with External Data

The Level2 vertical profiles analysed here have been processed with gopr v6.0a (IPF version 5.0), which includes Tikhonov regularisation and Global Doas Inversion on NO_2 and NO_3. We present here correlations between air density values measured by GOMOS and air density values from ECMWF, for different altitude ranges; O_2 concentration values measured by GOMOS and O_2 concentration values from ECMWF; and O_2 concentration values measured by GOMOS and O_2 concentration values inferred from GOMOS air density profiles. Detailed results of the reprocessed cycle 22 are presented, then results for all reprocessed cycles (cycles between 14 and 22) are summarized. Only full dark occultations are included in the calculations. The number of full dark occultations for each cycle is detailed in the table 7.1-1.

Table 7.1-1: Number of full dark occultations for reprocessed cycles between 14 and 22

Cycle number	Number of full dark occultations
14	3015
15	2592
16	511
17	1128
18	2963
19	3287
20	3997
21	2807
22	4869

7.1.1 AIR DENSITY AND O_2 VERTICAL PROFILES FOR CYCLE 22 (ORBITS BETWEEN 9073 AND 9573; 24/11/2003; 29/12/2003)

Fig. 7.1-1 illustrates the correlation between values of GOMOS air density and values of ECMWF air density, for altitudes between 25km and 35km. The correlation is good, with a correlation coefficient equal to 0.93. This correlation remains good, when calculated at lower levels of the stratosphere between 20km and 30km (fig. 7.1-2: correlation coefficient equal to 0.94 between 20km and 30km), and in the higher part of the stratosphere (fig. 7.1-3: correlation coefficient equal to 0.91 between 40km and 60km).

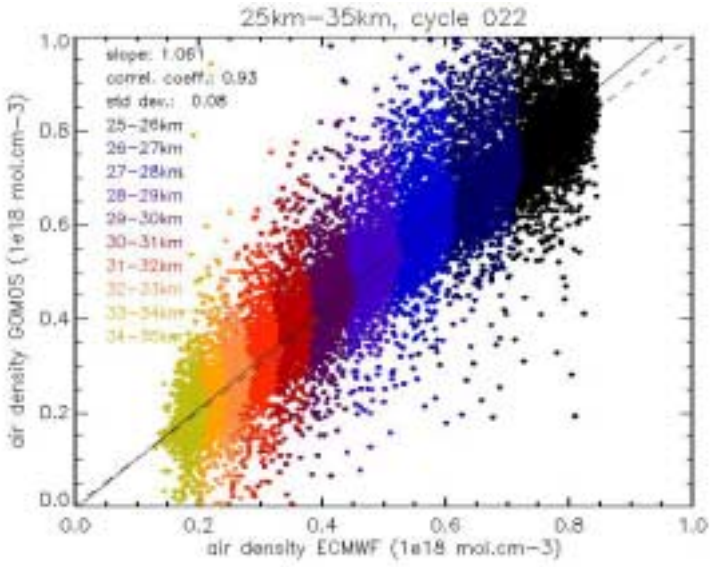

Figure 7.1-1: Correlation between values of GOMOS air density and values of ECMWF air density, for altitudes between 25km and 35km, measured for cycle 022. The solid line plots the linear fit to the data

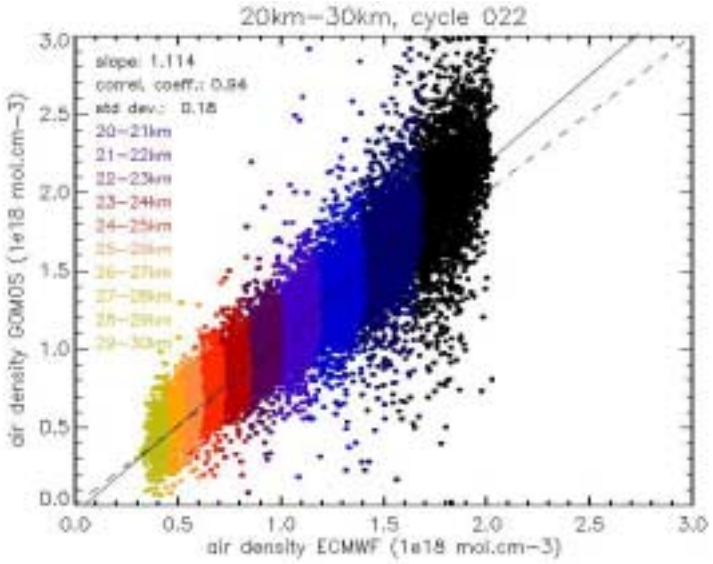

Figure 7.1-2: Correlation between values of GOMOS air density and values of ECMWF air density, for altitudes between 20km and 30km, measured for cycle 022. The solid line plots the linear fit to the data

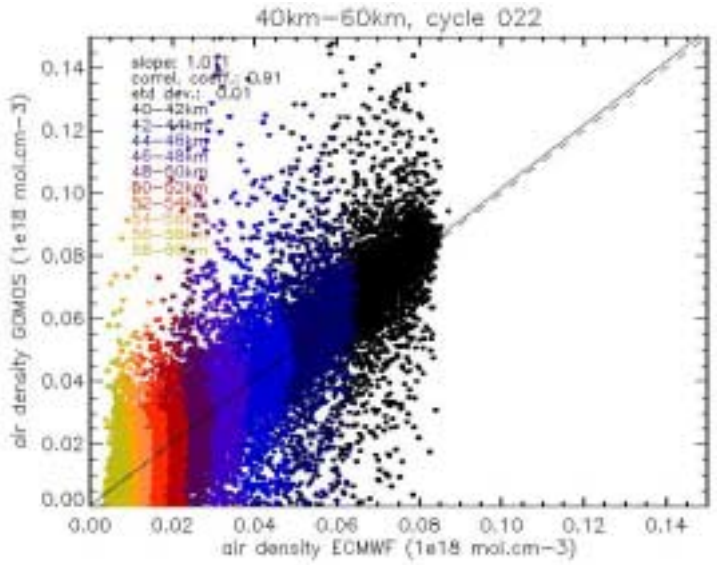

Figure 7.1-3: Correlation between values of GOMOS air density and values of ECMWF air density, for altitudes between 40km and 60km, measured for cycle 022. The solid line plots the linear fit to the data

Fig. 7.1-4 illustrates the correlation between values of GOMOS O_2 concentration and values of ECMWF O_2 concentration, for altitudes between 25km and 35km. The ECMWF O_2 vertical profile is reconstructed as 0.21 * ECMWF air density profile.

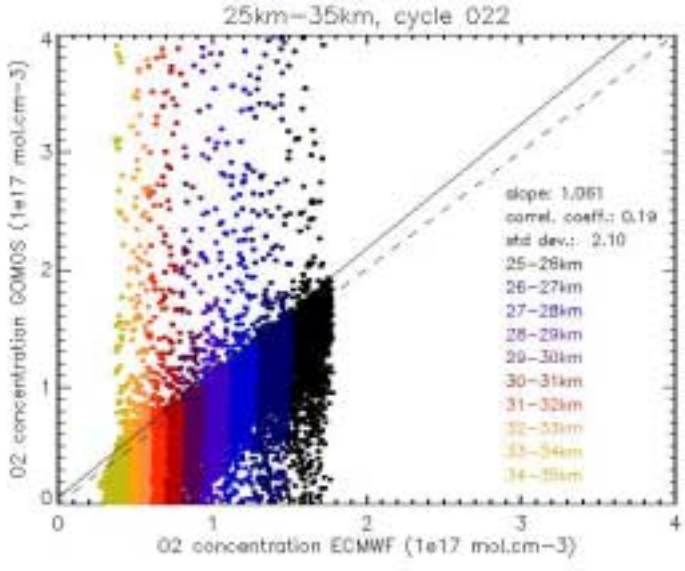

Figure 7.1-4: Correlation between values of GOMOS O_2 concentration and values of ECMWF O_2 concentration, for altitudes between 25km and 35km, measured for cycle 022. The solid line plots the linear fit to the data

The low correlation calculated between the two quantities in this case (correlation coefficient of 0.19) has been previously observed on similar datasets encompassing measurements at all latitudes and from all stars, whereas the correlation calculated on measurements from star 029 at low latitudes only (orbits between 3959 and 5093) was much higher (see the monthly report on January 2004 period). This will be

further investigated, in order to detect if this very low correlation between the two quantities in this case may be due to the global latitude coverage of the measurements taken into account, or to the many stars considered here.

Fig. 7.1-5 illustrates the correlation between values of GOMOS O_2 concentration and values of GOMOS O_2 concentration reconstructed as 0.21 * GOMOS air density profile, for altitudes between 25km and 35km. As for the previous figure, the high variability of O_2 GOMOS values for specific profiles is associated to a low correlation coefficient (0.16), and this will be also further investigated to detect any possible influence of the latitude and/or the star.

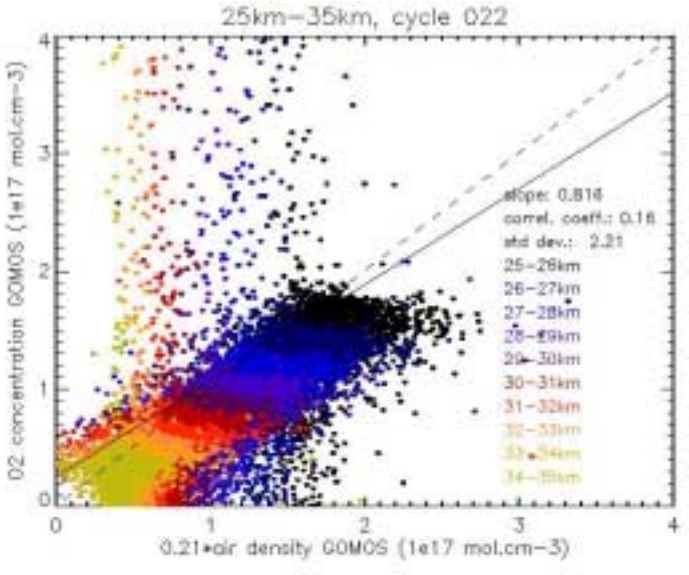

Figure 7.1-5: Correlation between values of GOMOS O_2 concentration and values of GOMOS O_2 concentration calculated as 0.21* GOMOS air density profile, for altitudes between 25km and 35km, measured for cycle 022. The solid line plots the linear fit to the data

7.1.2 RESULTS FOR ALL CYCLES

For all cycles reprocessed (between cycle 14 and cycle 22), results of the correlation are summarised in the table 7.1-2. Except for cycle 17, all cycles show a good correlation between air GOMOS and air ECMWF values between 20km and 30km with correlation coefficients higher than 0.85 (or than 0.92 when excluding cycle 18). The number of full dark occultations of cycle 17 is one of the lowest of all cycles (with cycle 16, see table 7.1-1), which might induce a statistical effect on the correlation. Between 25km and 35km, the correlation coefficients are higher than in the lower altitude range, between 0.91 and 0.96. In the higher stratosphere, cycle 16 shows the lowest coefficient (0.68). Coefficients for other cycles are higher than 0.84.
Similarly to cycle 22, the coefficients of the correlation between O_2 GOMOS and O_2 ECMWF values for altitudes between 25km and 35km are low (between 0.19 and 0.35) and values of the standard deviation are high (between 1.19 and 2.39). This is also the case for the correlation between O_2 GOMOS and 0.21*air density GOMOS values (correlation coefficients between 0.16 and 0.29; standard deviation values between 1.29 and 2.51).

Table 7.1-2: Correlation coefficients and standard deviation values for reprocessed cycles between 14 and 22

Cycle number	air 20-30km (GOMOS/ECMWF)		air 25-35km (GOMOS/ECMWF)		air 40-60km (GOMOS/ECMWF)		O_2 25-35km (GOMOS/ECMWF)		O_2 25-35km (GOMOS)	
	corr.coeff.	std. dev.	corr.coeff.	std. dev.	corr.coeff.	std. dev.	corr.coeff.	std. dev.	corr.coeff.	std. dev.
14	0.94	0.20	0.96	0.06	0.94	0.01	0.31	1.21	0.28	1.29
15	0.95	0.17	0.96	0.06	0.93	0.01	0.30	1.30	0.27	1.36
16	0.96	0.15	0.93	0.08	0.68	0.01	0.19	1.68	0.16	1.83
17	0.66	0.57	0.91	0.10	0.89	0.01	0.35	1.19	0.29	1.29
18	0.85	0.28	0.94	0.07	0.88	0.01	0.24	1.88	0.21	2.00
19	0.92	0.20	0.91	0.09	0.84	0.01	0.24	1.84	0.20	2.02
20	0.95	0.17	0.94	0.07	0.88	0.01	0.22	2.04	0.20	2.08
21	0.95	0.17	0.94	0.07	0.94	0.01	0.20	2.39	0.16	2.51
22	0.94	0.18	0.93	0.08	0.91	0.01	0.19	2.10	0.16	2.21

7.1.3 GOMOS O_3 CLIMATOLOGY IN 2003

The latitudinal variation of the vertical profiles of O_3 concentration in 2003 is plotted on fig. 7.1-6, for altitudes between 5km and 40km. Only measurements with a solar zenith angle higher than 110° have been included.

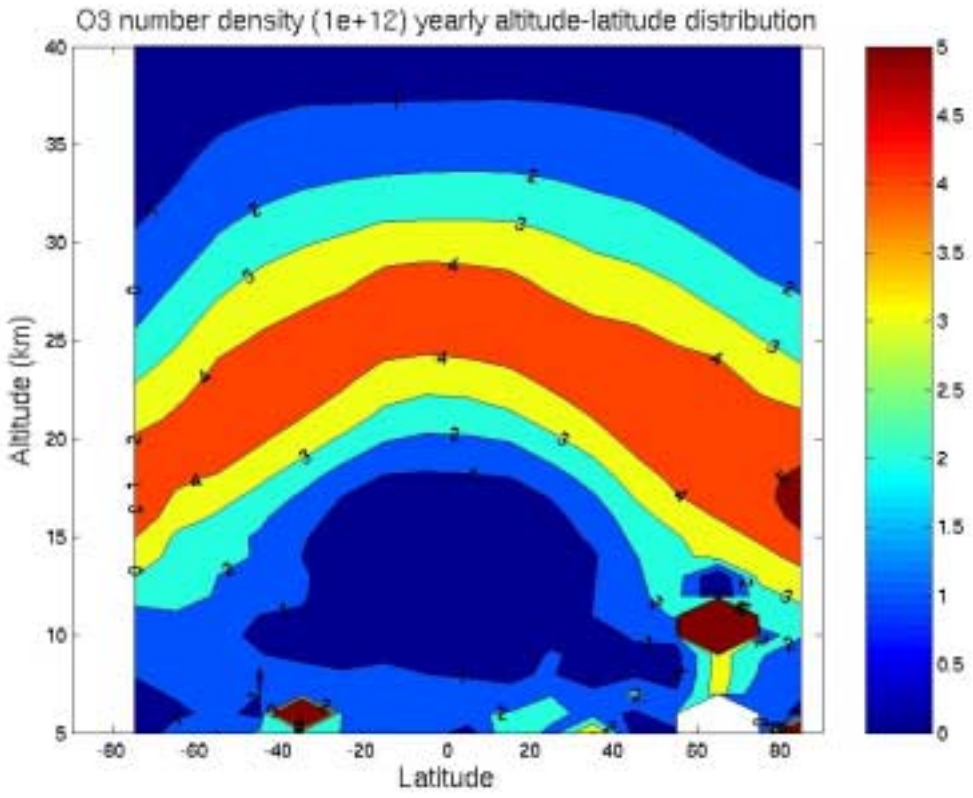

Figure 7.1-6: Altitude/latitudinal distribution of the GOMOS O_3 vertical profiles between 5km and 40km. O_3 values are plotted in concentration and correspond to all profiles measured in 2003 with a solar zenith angle higher than 110°

The results show the descent of the iso-surfaces from the low latitudes to the high altitudes. The maximum of 4.10^{12} molec cm^{-3} is located between 25km and 28km at low latitudes, and between 15 and 20km and high altitudes. The effect of some outliers can be noted below 8km, or up to 12km at high latitudes.

The latitudinal variation of the vertical profiles of O_3 mixing ratio in 2003 is plotted on fig. 7.1-7. As for the previous figure, only measurements with a solar zenith angle higher than 110° have been included. A maximum of 9 ppmv is retrieved at the Equator around 30km whereas it is equal to 4 or 5 ppmv at high latitudes. At highest altitude levels of the vertical profiles, the figure also shows a strong latitudinal variation of O_3 values. It illustrates the ability of GOMOS to capture the second ozone maximum at altitudes higher than 80km with a maximum at the Equator of 9 ppmv.

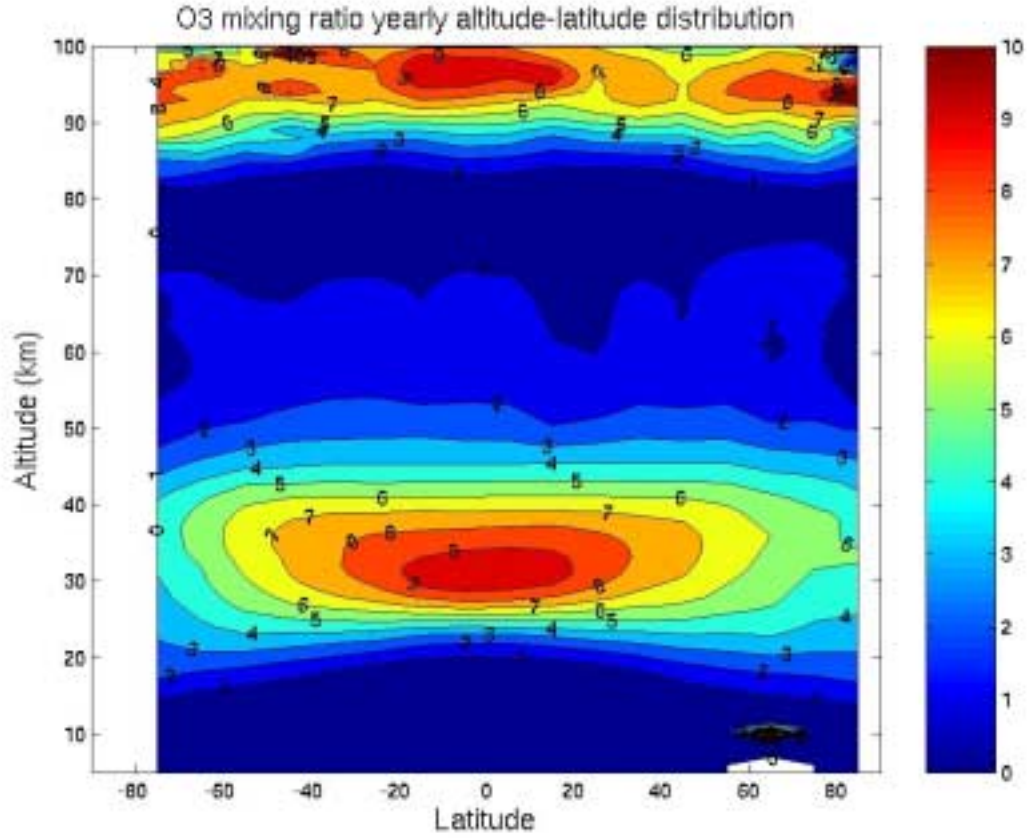

Figure 7.1-7: Altitude/latitudinal distribution of the GOMOS O_3 vertical profiles between 5km and 100km. O_3 values are plotted in mixing ratio and correspond to all profiles measured in 2003 with a solar zenith angle higher than 110°

7.2 GOMOS-Climatology Comparisons

Results will be presented upon availability.

7.3 GOMOS Assimilation

Results will be presented upon availability.

7.4 Consistency Verification: GOMOS-GOMOS Inter-comparison

Results will be presented upon availability.